NUREG/CR--4221

TI85 012540

An Evaluation of Stress Corrosion Crack Growth in BWR Piping Systems

Manuscript Completed: January 1984
Date Published: May 1985

Prepared by
M. Kassir, S. Sharma, M. Reich, M.-T. Chang

Brookhaven National Laboratory
Department of Nuclear Energy
Upton, NY 11973

Prepared for
Division of Engineering
Office of Nuclear Reactor Regulation
U.S. Nuclear Regulatory Commission
Washington, D.C. 20555
NRC FIN A3739

Blank Page

EXECUTIVE SUMMARY

Intergranular stress corrosion cracking and sub-critical growth in typical BWR 304 stainless steel pipes are reviewed and discussed. Attention is focused on identifying the parameters that have major influence on the growth behavior of pre-existing flaws under normal operating conditions. These parameters include: (1) Applied and residual stresses as characterized by their corresponding stress intensity factors, (2) Sensitization of the base metal in the heat affected zone adjacent to girth welds, and (3) The continuous exposure of the material to an environment of high temperature water containing dissolved oxygen and diluted levels of sulfate and chloride impurities. Sensitivity study of the influence of these parameters on the time required for a stress corrosion crack to reach a critical size is performed in order to ascertain their role and importance on growth behavior.

The major accomplishments and conclusions reached in this study are:

(1) Stress Intensity Factors: The available techniques and formulations for computing the stress intensity factors of surface cracks in pipes were reviewed and assembled in the report. The assembled data included k-factors for both full- and part-circumferential cracks as well as axial cracks. For identical loadings the k-factor of a partial-circumferential crack is always less than the corresponding value of the complete circumferential crack. Thus, the use of the latter value will insure conservative growth characteristics for these types of cracks.

(2) Operating Stress: Crack growth depends on the combination of k-factors due to operating and residual stresses. As long as the sum is positive there will be crack growth. For this study typical operating stress values for various pipe sizes given in the literature were used for crack growth calculations. Variations of operating stress and their effects on the crack growth in representative piping systems are being studied.

(3) Residual Stress and Pipe Geometry Effects: The pattern of residual stress distribution across the thickness due to welding has a major influence on crack growth. For large diameter pipes (diameter 26-28" with thickness 1-3/8"), significant variations in the residual stress distribution have been

reported. As discussed in the text, for some distributions the total k-factor can become negative at some crack depth and thus arrest further crack growth. For other distributions of residual stress, however, there is continuous crack growth (see Figs. 22 and 23), with varying time estimates to code allowable crack size depending on initial crack depth and applied crack growth law. It is the authors opinion, that the latter residual stress distributions are more realistic, and complete crack arrest is unlikely to occur. As can be observed from the above mentioned figures, for detected flaws with initial depth to thickness ratios of 10 to 20 percent, there is a large range for the predicted life. Considering only the average crack growth laws, the predicted life to code allowable size, would range from approximately 40 to 100 months, while the most conservative crack growth law would yield a time range of 10 to 60 months. For deeper initial cracks, lifetimes will be shorter and time ranges due to different residual stress assumptions will also be less. These factors must be considered in order to establish an effective inspection and repair schedule.

In small diameter pipes available data indicates that the residual stress always has an aggravating effect, in that it accelerates crack growth. Life estimates for these pipes are displayed in figures 24 and 25. From the results, it is recommended that these pipes be repaired or replaced as soon as flaws are detected.

(4) Environment and Water Chemistry: The degree of sensitization in the base metal near a weld joint (where intergranular cracks are detected) has a great influence on the expected time for subcritical crack growth. Faster growth (by an order of magnitude or higher) has been achieved in the laboratory by utilizing test specimens with a higher level of sensitization. There is some data which suggests that the degree of sensitization in a weld joint of an operating BWR pipe increases with time and can lead to accelerated cracking.

The amount of dissolved O_2 concentration influences crack growth rate when it is below 1 ppm but does not seem to have an affect above that level. In addition, there is evidence which indicates that dilute levels of impurities (sulfates and chlorides) present in the water can increase growth time.

Recommendations

The above accomplishments and conclusions are based on the original work scope envisioned for this task. Based on the outcome of this study, the following recommendations can be made:

(a) As detailed in the report, the distribution of the weld residual stress across the thickness in large diameter pipes cannot be adequately determined from existing literature data. Considering that crack growth or its arrest is greatly influenced by the residual stress k-factor, it is recommended that a detailed analytical study be carried out to determine the important parameters affecting the residual stress distributions and their corresponding k-factors. Furthermore, a review should be made of experimental methods that would allow the determination of actual residual stresses. When combined with the metallurgical aspects, this study could result in the identification of the most optimum welding conditions that would lead to favorable residual stress distributions and degree of material sensitization.

(b) Weld overlays were not included in this phase of the BNL Work Scope. Since this technique (which again involves weld residual stresses) is one of the major components of the repair program, its effects with respect to stress redistribution and consequent crack growth or arrest need detailed study.

(c) In the study k-factors for fully circumferential cracks were used in order to obtain conservative time estimates for growth. Some calculations using k-factors for partially circumferential cracks should also be made for comparative purposes.

(d) As mentioned, typical operating stress values for various pipe sizes were taken from the literature. In order to evaluate the variations inherent in the operating stresses and their effects on crack growth, it is recommended that a stress calculation be performed for a typical piping system. This is a relatively simple and straight forward task if piping system data is available.

ACKNOWLEDGEMENTS

This work was supported by the U.S. Nuclear Regulatory Commission under FIN No. A-3739. The advice, support and encouragement during various phases of this work given by Mr. C.Y. Cheng and Mr. R.H. Vollmer of the Office of Nuclear Reactor Regulation are gratefully acknowledged. The authors want to express their thanks to Ms. Joan Murray for typing this report.

TABLE OF CONTENTS

		Page
EXECUTIVE SUMMARY		iii
ACKNOWLEDGEMENTS		vi
LIST OF FIGURES		viii
LIST OF TABLES		x
I.	INTRODUCTION	1
II.	STRESS INTENSITY FACTORS FOR PART-THROUGH INTERNAL SURFACE CRACKS IN PIPES	3
	A. Complete Circumferential Cracks	4
	B. Long Axial Cracks	24
	C. Semi-Elliptical Part-Through Axial and Circumferential Cracks	24
III.	EXPERIMENTAL CRACK GROWTH RATES	30
IV.	EVALUATION OF CRACK GROWTH IN WELDED BWR PIPING SYSTEM	45
V.	SUMMARY COMMENTS	57
VI.	CONCLUSIONS	60
REFERENCES		63

List of Figures

Figure		Page
1	A Pipe Containing an Axisymmetric Circumferential Crack	6
2	Stress Intensity Factor for a Small Crack Depth (L/h = 0.01) in a Cylinder Subjected to Axial Tension	7
3	Self-Equilibrating Axial Residual Stress	10
4	Stress Intensity Factors for Circumferential Cracks in Hollow Cylinder Subjected to Residual Stresses	10
5	Stress Intensity Factor for a Cracked Pipe Subjected to Uniform Axial Stress, a/b = 0/91 (obtained by numerical integration of weight functions, Ref. 4)	13
6	Residual Axial Stress (dotted curve) and Resulting k-factor (a/b = 0.91)	15
7	Magnification Factors for a Circumferential Crack in a Pipe with a/b = 0.91 (Refs. 4 and 9)	16
8	Through-Wall Residual Stress Measurements on 28-in Diameter Pipe (ANL, Ref. 7)	19
9	Typical Distribution of Through-Wall Weld Residual Stress (S = 30 ksi)	22
10	Axial Residual Stress Distribution (pipe diameter of 20 to 28 in, Ref. 11)	23
11	Geometry of Long Axial Cracks in Pipes	26
12	Magnification Factors for Part-Through Axial Cracks (a/L = 10)	27
13	Geometry of Semi-Elliptical Longitudinal Crack	29
14	Magnification Factors for a Semi-Elliptical Longitudinal Flaw in a Pipe (a/b = 0.91, L/h = 0.25, c/L = 3)	31
15	Magnification Factors for a Semi-Elliptical Longitudinal Flaw in a Pipe (a/b = 0.91, L/h = 0.50, c/L = 3)	32
16	Magnification Factors for a Semi-Elliptical Longitudinal Flaw in a Pipe (a/b = 0.91, L/h = 0.8, c/L = 3)	33

List of Figures (Cont'd)

Figure		Page
17	Semi-Elliptical Part-Through Circumferential Crack	
18	Summary of Constant Load Crack Growth Data (Curves are evaluation curves). Data collected in 0.2 ppm O_2 and 8 ppm O_2 water. Different levels of sensitization examined	34 40
19	Constant Load Crack Growth Rates Measured as a Function of Stress Intensity Factors	41
20	Crack Growth Rates vs. Stress Intensity Factors (ANL, 23) ..	42
21	Crack Growth Rate of Sensitized 304 Steel	44
22	Crack Growth for 28 in. Pipe - Residual Stress Case (A)	49
23	Crack Growth in 28 in. Pipe - Residual Stress Case (B)	50
24	Crack Growth for 4 in. Pipe	53
25	Crack Growth for 12 in. Pipe	55

List of Tables

Table		Page
1	Values of $k/\sigma_0 (\pi L)^{1/2}$ for an Internal Edge Crack in a Thick-Walled Cylinder Subjected to Axial Tension	8
2	Effect of Poisson's Ratio on the Values of the K-factor. a/b = 0.5, L/h = 0.3	8
3	Values of $k/\sigma_0 (\pi L)^{1/2} \cos\theta$ for a Circumferential Edge Crack in a Cylinder Subjected to Pure Bending	11
4	Effect of Poisson's Ratio on the Values of the K-factor (Pure Bending) a/b = 0.5, L/h = 0.3	11
5	Stress Intensity Factors for Axial Residual Stress - 28" Pipe	18
6	Stress Intensity Factors for Residual Stress Measurements Shown in Figure (8)	20
7	Stress Intensity Factors for Axial Residual Stress in Figure (9)	20
8	Stress Intensity Factors for Residual Stress Shown in Figure (10) - 28" Pipe	25
9	Total Stress Intensity Factors in Large Diameter BWR Pipes (28" Diameter) - ksi $\sqrt{\text{in.}}$	48
10	Stress Intensity Factors in Small Diameter Pipes	56

I. INTRODUCTION

Over the last few years, intergranular stress corrosion cracks (IGSCC) have been observed in BWR piping systems. The cracks were detected in both the axial as well as the circumferential directions. They initiate from the inside surface of the heat affected zone adjacent to girth welds. The crack growth is believed to be due to the influence of the following simultaneous factors: (1) the action of applied loading and sustained stresses: (2) sensitization of the material in the vicinity of the weld zone and (3) the continuous exposure of the material to an environment containing high temperature water ($\approx$ 290°C), dissolved oxygen ($\approx$ 0.2 ppm), and some low levels of sodium chloride and sodium sulfate. -Under normal operating conditions, the loads are essentially those due to internal pressure, dead weight, thermal expansions and residual stresses. The cyclic thermal transients are usually ignored since they do not contribute significantly to corrosion fatigue crack growth.

A chromium depletion model has been suggested to explain the origin of IGSCC in the pipes. Briefly, this model can be explained as follows: When the metal is subjected to substantial thermal treatment (as during welding), the chromium - originally added to the material to prevent corrosion - interacts with any carbon in the solution and forms chromium carbides. These carbides in turn, precipitate at the grain boundaries and deplete the metal from the protective chromium oxide shield. Thus, corrosion cracks initiate at the grain boundaries, and the steel is said to be 'sensitized'. Moreover, the chromium depleted zones provide a preferential path for the cracks to propagate and additional cracking seems to occur when the region is exposed to substantial stress in the presence of oxygenated high temperature water and diluted amounts of impurities.

For circumferential cracks (which are the focus of most of the BWR pipe crack investigations) the most critical questions to be answered are: How long will it take for a detected flaw to propagate through the wall thickness?

And would the flaw eventually cause a leak in the pipe before total severance? These are important questions because of the safety consequences and the costs involved in carrying out inspections and/or repair to the piping systems.

The first task in the evaluation of the growth of any crack is the determination of the crack growth driving force or the stress intensity factor under service and extreme conditions. For internal circumferential cracks in pipes, the stress intensity factors due to axial stresses control the crack growth process. Section II of this report contains a comprehensive compilation of numerical values for the stress intensities or the so-called k-factors obtained by various elastic techniques. Since the k-factor of a partial circumferential surface crack in a pipe is less than the corresponding value of a complete circumferential crack, the use of the latter values yield conservative growth characteristics and at the same time simplify the analysis considerably. The total axial stresses to be considered include those generated by the applied stresses (internal pressure, dead weight and thermal expansion due to start up or shut down thermal transients) and residual stresses. The other transient stresses (associated with normal operation and emergency events) produce small fatigue crack growths and thus can be neglected. Consistent with linear elastic methods, the resulting stress distributions can be superimposed to compute the largest k-factor. The k-factors for the applied stresses can be found in the tables and charts provided in Section II. The distribution of the residual stress is highly non-linear and is influenced by a number of variables (welding procedure, thermal treatment, pipe thickness, etc.); hence, numerical techniques such as the finite element methods or integration of the influence functions are resorted to for obtaining the stress-intensity factors. Some examples of typical distributions of residual stress in large and small diameter pipes and their resulting stress intensity factors are given in Section II.

The next step in the process of evaluating stress corrosion crack growth is to perform fracture mechanics type of tests in order to measure crack

propagation rates as functions of the stress intensity factors under the environment and loading conditions prevailing in typical BWR installations. Normally the piping system operating conditions involve steady state loadings and an environment consisting of a concentration of 0.2 ppm of oxygen in pure water at a temperature of 290°C. The most common type of tests utilize compact tension or cantilever bend specimens. It is known that several factors affect the rate of crack growth. These include material condition (degree of sensitization), loading history, and environment (water chemistry and temperature). Section III of this report contains a critical review of the available experimental data that was used in order to explore the influence of these factors. Various crack growth formulas which correspond to upper and lower bounds as well as intermediate data are developed.

Finally, in Section IV of this report, the aforementioned formulas are employed to compute the predicted rates of growth of typical flaws in BWR pipes of various sizes (28-inch, 12-inch and 4-inch diameters). The computation is illustrated by comparing the influence of using the various numerical values of the k-factors presented in Section II and the fracture mechanics growth formulas developed in Section III. Since the aim of this work is to perform an assessment of the effects of stress intensity factors and environment on the behavior of IGSCC in type 304 stainless steel, a sensitivity study is performed to identify the influence of the important parameters (e.g., patterns of residual stresses, extreme - i.e., bounds - and intermediate data based crack growth formulas, initial size and orientation of detected flaws, pipe size, etc.) on the predicted time that it takes a given flaw to reach the code allowable size.

II. STRESS INTENSITY FACTORS FOR PART-THROUGH INTERNAL SURFACE CRACKS IN PIPES

The redistribution of stress in a pipe due to the presence of cracks or defects may initially be assessed by employing the methods of linear elastic analysis. Of course the greatest emphasis should be placed on determining the stress concentration near the crack tip. This elevation of stress can be measured by the stress intensity factor, k (in the literature, the symbol k_1, is often used to denote "opening mode" of crack surfaces). Physically,

the k-factor can be viewed as the intensity of the load transmitted through the crack tip region due to the introduction of the crack into the pipe. The k-factor of a given problem is usually determined by solving certain boundary-value problem in the mathematical theory of elasticity with special emphasis on the state of stress near the crack edge. In this section we present a literature review of current stress intensity factor data applicable to crack growth rates in sensitized stainless steel pipes. The crack geometries that are considered can be conveniently grouped into three main categories:

A. Complete Circumferential Cracks

B. Long Axial Cracks

C. Semi-Elliptical Part-Through Axial and Circumferential Cracks

Wherever possible, the numerical values of the k-factor due to the relevant stresses operating at the crack surfaces will be given and the references from which they are obtained will be stated to enable further study. It is to be noted that since the stress intensity factors are obtained by performing linear analysis, direct superposition of the results can be utilized, i.e., the k-values can be added for different fields of stress provided that they belong to the same mode of crack opening. Furthermore, the formulas for the stress intensity factors can be combined with the material characteristics to perform calculations of subcritical crack growth and fracture mechanics analysis of stress corrosion crack growth in austenistic stainless steel used in BWR pipes.

A. Circumferential Cracks:

The circumferential cracks in BWR pipes have been observed to have a large length (along the circumference) to depth ratios. Thus, they can be conservatively assumed to be completely circumferential. This assumption greatly simplifies the stress analysis of the problem. Analytical as well as numerical methods (such as the boundary integral equations and finite elements) have been used to determine the stress intensity factor for various loadings across the crack plane.

ANALYTICAL METHODS

In Reference [1], Nied and Erdogan considered the elasticity problem of a long hollow circular cylinder containing an axisymmetric internal circumferential crack subjected to general non-axisymmetric loading. Figure (1) shows a longitudinal cross section of the pipe where the inner and outer radii of the cylinder are denoted by a and b, respectively, and the crack is assumed to have a length L = d - a where d is defined in the figure. The geometry of the problem is described by cylindrical coordinates (r, θ, z) with the origin located at the center of the crack plane and the z-direction along the axis of the pipe. The problem is formulatd in terms of a system of singular integral equations with the Fourier coefficients of the derivative of the crack surface displacement as the density function. The integral equations are solved numerically and the stress intensity factor along the crack edge r = d, which is defined by the relation

$$k = \lim_{r \to d} \sqrt{2\pi(r-d)} \quad \sigma_z(r, \theta, o) \quad , \qquad (1)$$

is computed for three different loading conditions: A uniform axial stress, bending by end couples, and a self-equilibrating residual stress.

UNIFORM AXIAL STRESS

For this case, it is assumed that the crack surfaces are opened by the application of a uniform axial stress σ_0 (where $\sigma_0 = p_\infty/\pi\ (b^2 - a^2)$ and p_∞ = the axial tension) to its surfaces. Table (1) presents the numerical values of the k-factor for various ratios a/b and L/h where h represents the thickness (i.e., = b - a). Poisson's ratio (ν) of the material is assumed to be 0.3. It is clear from the table that the stress intensity factor is a monotonously increasing function of a/b for all crack depths. The limiting values of k for (a/b) $\to$1 shown in the table are obtained from the plane strain solution of a strip containing an edge crack[2]. For a very small crack depth (i.e., L/h = 0.01) effect of a/b on the variation of k is shown in Figure (2).

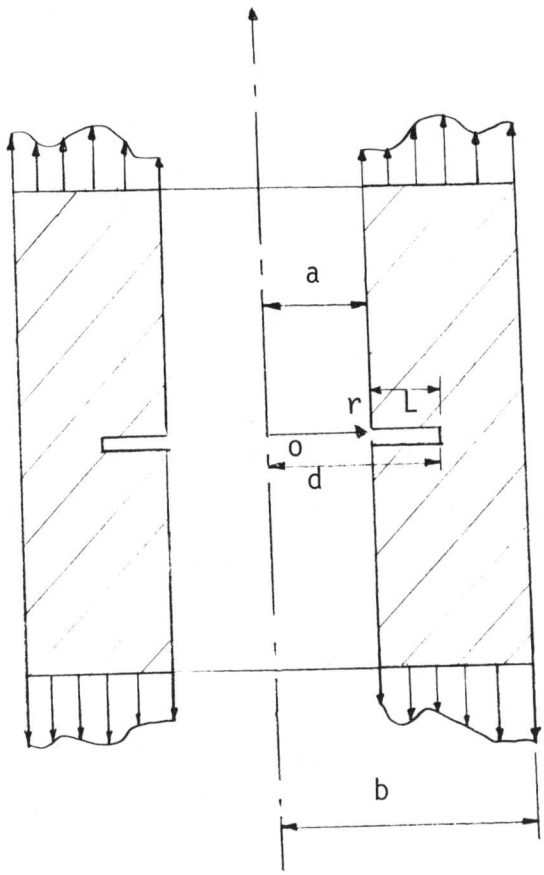

Fig. 1 A Pipe Containing an Axisymmetric Circumferential Crack.

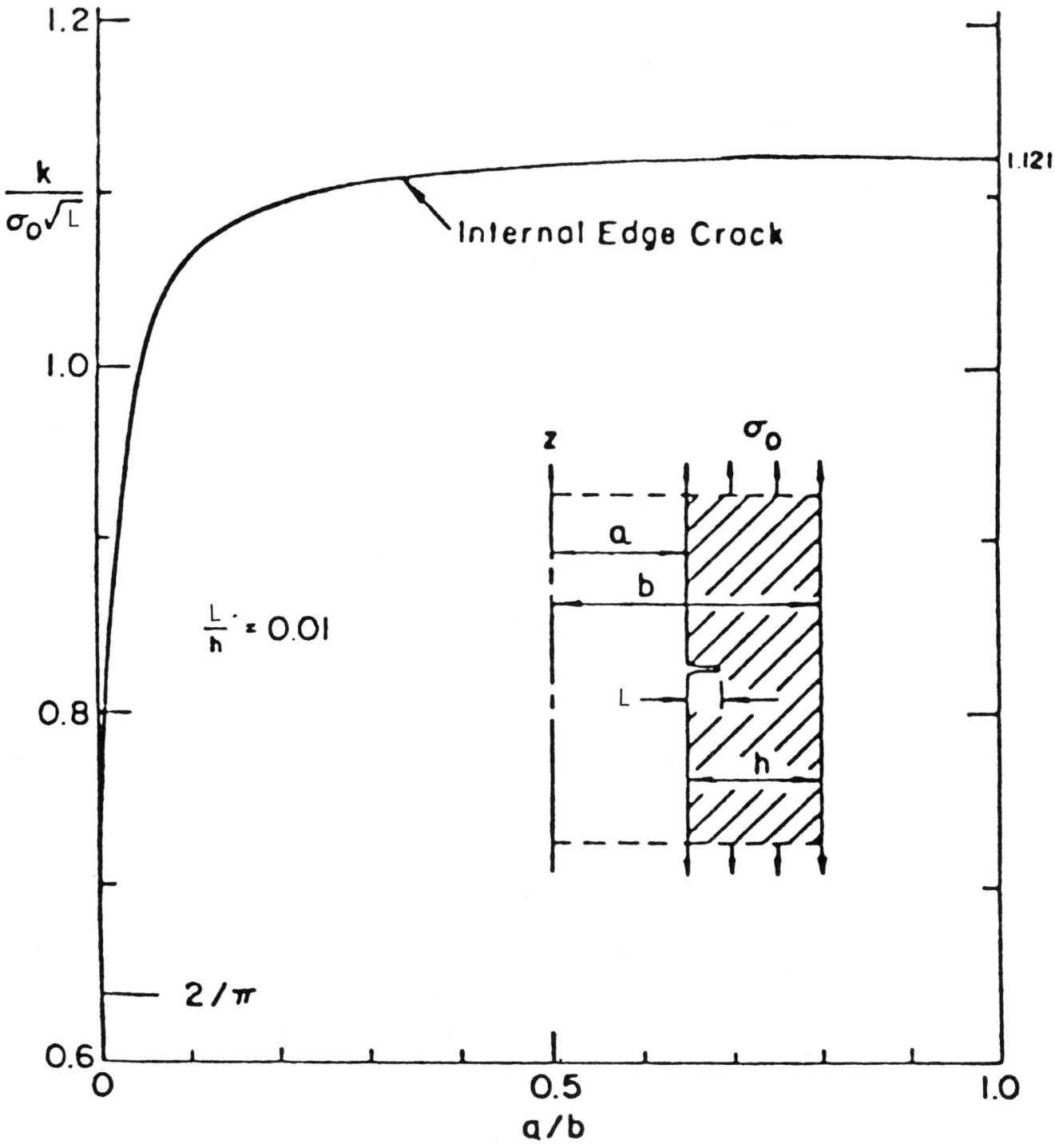

Fig. 2 Stress Intensity Factor for a Small Crack Depth (L/h = 0.01) in a Cylinder Subjected to Axial Tension.

Table (1): Values of $k/\sigma_0(\pi L)^{1/2}$ for an Internal Edge Crack in a Thick-Walled Cylinder Subjected to Axial Tension.

a/b	L/h					
	0.1	0.2	0.3	0.4	0.5	0.6
0	0.637	0.644	0.651	0.665	0.691	0.736
0.1	0.842	0.775	0.753	0.754	0.775	0.820
0.2	0.940	0.869	0.840	0.838	0.859	0.908
0.3	1.000	0.942	0.918	0.920	0.945	1.000
0.4	1.042	1.003	0.991	1.001	1.035	1.079
0.5	1.073	1.055	1.060	1.085	1.131	1.208
0.6	1.097	1.104	1.130	1.174	1.239	1.333
0.7	1.119	1.150	1.203	1.275	1.366	1.484
0.8	1.138	1.198	1.286	1.397	1.529	1.688
0.9	1.158	1.253	1.293	1.368	1.779	2.025
→1.0	1.189	1.367	1.660	2.112	2.826	4.035

Table (2): Effect of Poisson's Ratio on the Values of the K-factor.
a/b = 0.5, L/h = 0.3

ν	0	0.1	0.2	0.3	0.4	0.5
$K/\sigma_0\sqrt{\pi L}$	1.048	1.051	1.055	1.060	1.067	1.076

It is seen that as the values of (a/b) approach 0 and 1, $k/\sigma_0 (\pi L)^{1/2}$ approaches $2/\pi$ and 1.121, which respectively are the values for a penny-shaped crack in an infinite solid [3] and for a strip with an edge crack [2]. The effect of Poisson's ratio on the values of the stress intensity factor is indicated in Table (2) for the particular geometry of a/b = 0.5 and L/h = 0.3. It may be concluded that k increases monotonously, but very slightly with increasing Poisson's ratio.

PURE BENDING

When the pipe is bent by end couples (M), the crack surface stresses can be expressed as $\sigma_\theta(r,\theta,0) = \sigma_1(r/b)\cos\theta$, where $\sigma_1 = 4Mb/\pi (b^4 - a^4)$. It is assumed that the normal crack surface displacement, Uz $(r,\theta,0)$, everywhere in the crack region, is positive so that the stress intensity factor would also be positive for all values of θ. Table (3) shows the range of values of the stress intensity factors for different ratios of a/b and L/h (where ν is assumed to be 0.3). Table (4) reveals the effect of Poisson's ratios on the k-factor for the particular geometry of a/b = 0.5 and L/h = 0.3. As shown, the magnitude of the correction factor in the stress intensity factor is lower than the uniform axial stress loading case discussed previously.

RESIDUAL STRESS

For this loading condition, the crack surfaces are assumed to be under the action of self-equilibrating residual stress given by the formula

$$\sigma_0(r,\theta,o) = -\sigma_s \left[\frac{6(r-a)(b-r)}{(b-a)^2} - 1 \right] , \qquad (2)$$

where σ_s is the magnitude of the compressive stress on the surfaces of the cylinder. The variation of the axial stress given in Equation (2) is shown in Figure (3). It is parabolic in r, compressive on and near the surfaces, tensile in the inside region of the wall and statically self-equilibrating.

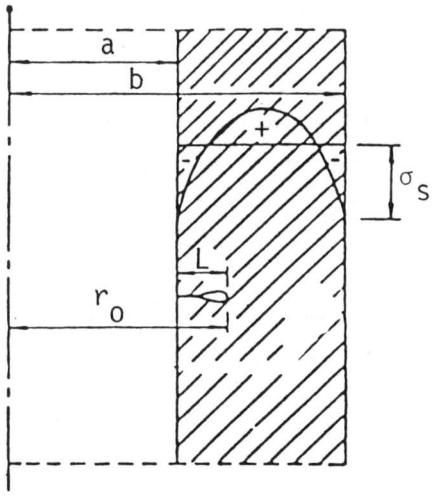

Fig. 3 Self-Equilibrating Axial Residual Stress.

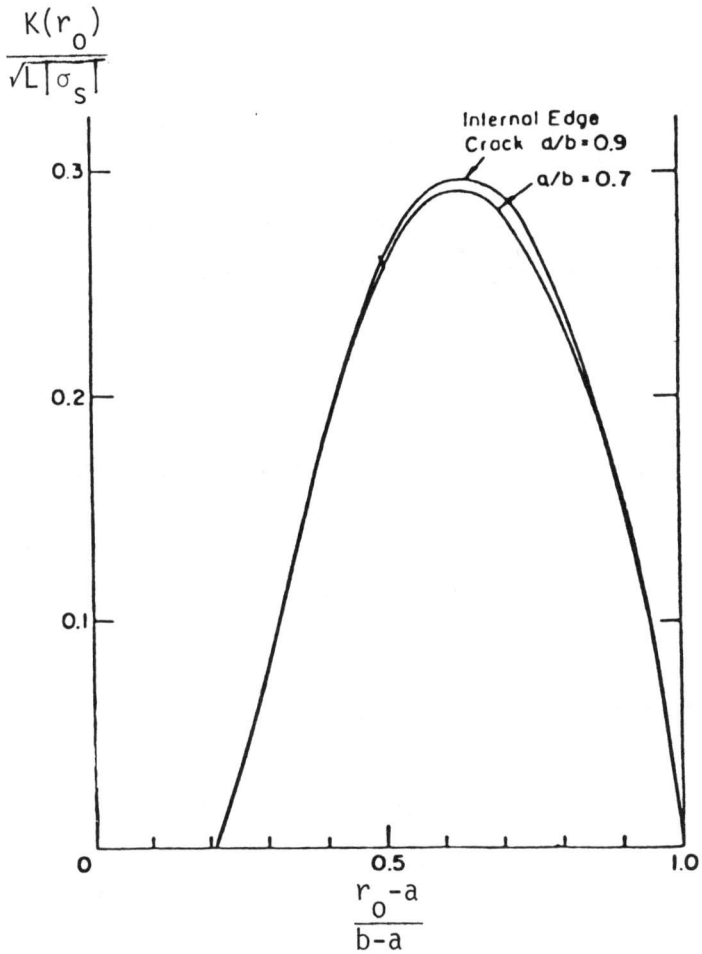

Fig. 4 Stress Intensity Factors for Circumferential Cracks in Hollow Cylinder Subjected to Residual Stresses.

Table (3): Values of $k/\sigma_1(\pi L)^{1/2}\cos\theta$ for a Circumferential Edge Crack in a Cylinder Subjected to Pure Bending.

a/b	L/h					
	0.1	0.2	0.3	0.4	0.5	0.6
0	0.042	0.085	0.127	0.171	0.217	0.265
0.1	0.123	0.153	0.188	0.226	0.267	0.314
0.2	0.225	0.241	0.266	0.296	0.333	0.378
0.3	0.334	0.342	0.359	0.383	0.415	0.459
0.4	0.447	0.452	0.466	0.487	0.517	0.561
0.5	0.563	0.571	0.587	0.611	0.643	0.691
0.6	0.680	0.698	0.724	0.757	0.799	0.856
0.7	0.800	0.833	0.876	0.928	0.989	1.066
0.8	0.922	0.978	1.053	1.141	1.243	1.359
0.9	1.048	1.139	1.267	1.426	1.612	1.824
→1.0	1.189	1.367	1.660	2.112	2.826	4.035

Table (4): Effect of Poisson's Ratio on the Values of the K-factor (Pure Bending) a/b 0.5, L/h = 0.3

ν	0	0.1	0.2	0.3	0.4	0.5
$\frac{k}{\sigma_1(\pi L)^{1/2}\cos\theta}$	0.574	0.577	0.582	0.587	0.594	0.602

The tensile region is defined by the relation $r_1 < r < r_2$ where $r_1 = a + 0.211\ (b-a)$ and $r_2 = a + 0.789\ (b-a)$. If the crack tip is located by the parameter r_o (see Figure 3), and if $r_o < r_1$ and $r_o > r_2$, then the crack lies in the compressive zones near the pipe surfaces and the crack surfaces would remain closed with k equal to zero. However, if $r_1 < r_o < r_2$, the crack tip is in the tensile zone and k is positive. For two cylinders with thickness ratios a/b = 0.7 and 0.9, Figure (4) shows the stress intensity factor $k\ (r_o)$. Note that k is positive in the region $r_1 < r_o < b$. Initially as the crack length L increases, k increases, and goes through a maximum and then tends to zero as the crack traverses the entire cylinder wall. It should also be realized that this is a crack-contact problem where the crack surfaces are partially closed (k = o). Further details are available in Reference [1].

NUMERICAL METHODS

The stress intensity factors for complete circumferential cracks in a straight pipe under the action of arbitrary axisymmetric stress in the pipe wall can also be evaluated by use of the weight functions given by Labbens, et al [4]. These weight functions are available for pipes with internal radius to thickness ratios of 10 and 5, i.e., a/b = 0.91 and 0.83 respectively. Harris [5] employed these weight functions to compute the stress intensity factor of a pipe with a/b equal to 0.91, under the action of uniform axial stress. These results are exhibited in Figure (5). For L/h = 0.4, $K/\sigma_o (\pi L)^{1/2} = 2.65$, whereas linear interpolation of the results in Table (1) gives a corresponding value of 2.55 (about 3.68% error).

Harris [5] also computed the stress intensity factor for a particular distribution of axial residual stresses across the pipe thickness. Finite element calculations of the residual stresses in a 71 cm (28 in.) pipe are available in Reference [6] which are in good agreement with the experimental measurements reported in Reference [7]. These finite element results can be conveniently summarized by the relation

$$\left.\begin{aligned} \sigma_{Res.}(r) &= \frac{a}{r}\,\sigma_R \cos\left[2\pi\left(\frac{r-d}{h}\right) + 60\right] \\ \sigma_R &= 317\ \text{MPa (46 ksi)},\ a = 12.74",\ h = 1.26" \end{aligned}\right\}, \qquad (3)$$

where the variable (r) is measured from the center of the pipe.

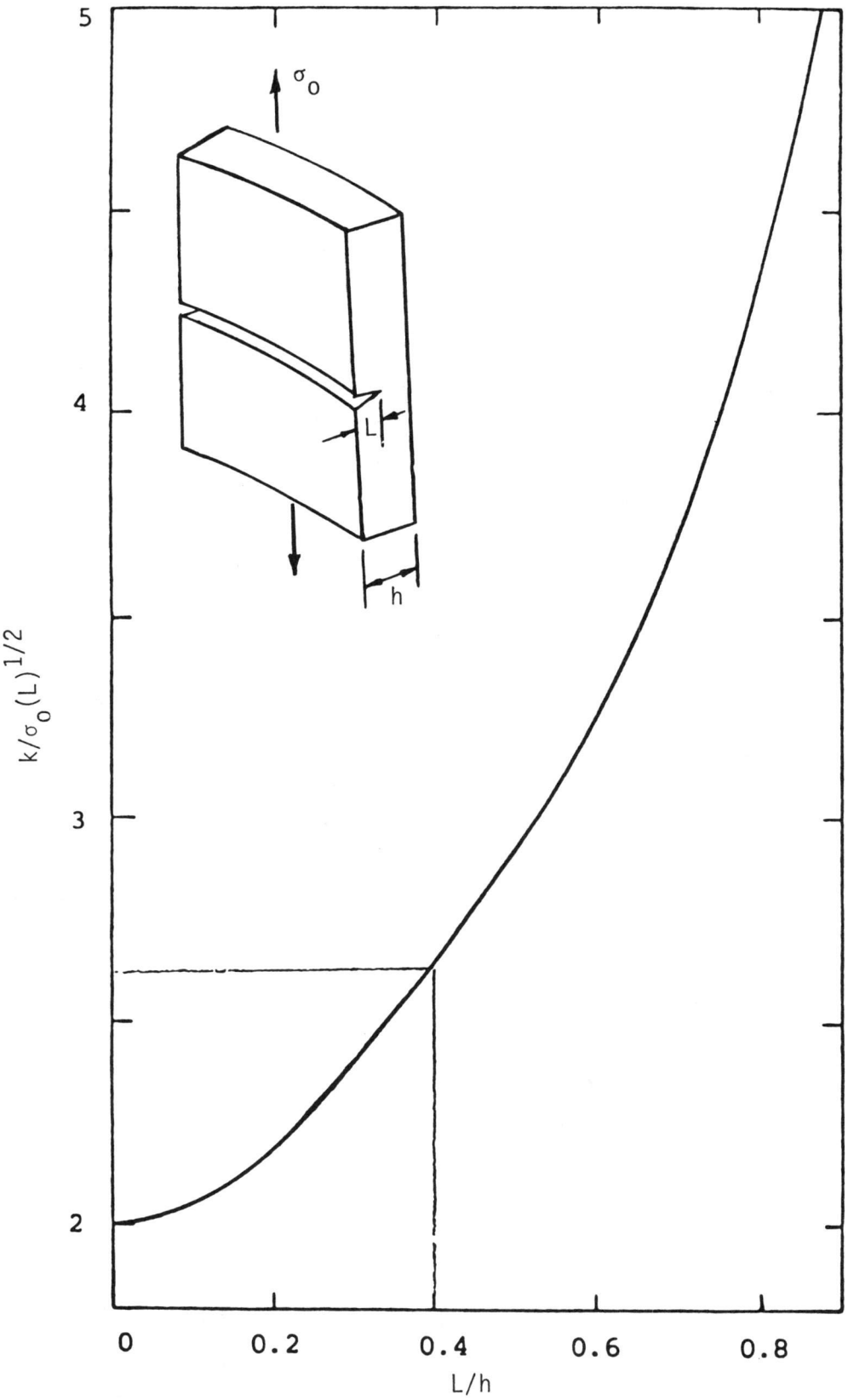

Fig. 5 Stress Intensity Factor For a Cracked Pipe Subjected to Uniform Axial Stress, a/b = 0.91 (obtained by numerical integration of weight functions, Ref. 4).

Equation (3) and the resulting stress intensity factor for a pipe with a/b = 0.91 are shown in Figure (6) which was obtained by numerical integration of the weight functions [5]. The figure reveals that k is negative over a large range of crack depth. Of course, the negative values of k are meaningless since when k = 0, the crack surfaces close and crack arrest results. Harris' method of obtaining the stress-intensity factor for a circumferential crack subjected to axisymmetric stresses has been coded on an electronic computer by using a FORTRAN subroutine called DRIVE. Instructions for the use of this subroutine is given in Reference [8], which includes description of the input and output parameters and few illustrative examples. This program as well as the results given in Figures (5) and (6), however, are applicable to pipes with a/b = 0.91 or 0.83 only, since they are based on numerical integration schemes employing Labbens weight functions [4] which are specifically derived for these ratios. Weight functions for other values of a/b can be constructed by the method described in Reference [4].

Stress-intensity factors for complete circumferential cracks in pipes and edge cracks in plates are also available and are described by Buchalet and Bamford [9]. These factors were developed by use of two-dimensional finite element methods. The stress profile across the crack surface is represented by a third degree polynomial

$$\sigma(X) = A_0 + A_1X + A_2X^2 + A_3X^3 \quad , \tag{4}$$

in which A_j (j = 0,1,2,3) are constants. The corresponding stress intensity factor is found to be given by the relation

$$k = (\pi L)^{1/2} \left[A_0F_1 + \frac{2L}{\pi} A_1F_1 + \frac{L^2}{2} A_2F_3 + \frac{4L^3}{3\pi} A_3F_4\right] \quad , \tag{5}$$

where L is the crack depth and F_j (j = 1,2,3,4) are magnification factors associated with the structural geometry of the cracked pipe. The variation of the magnification factors with the fractional distance through the pipe thickness (L/h) is shown in Figure (7). In addition, the same figure displays the corresponding results obtained by employing the boundary integral method of

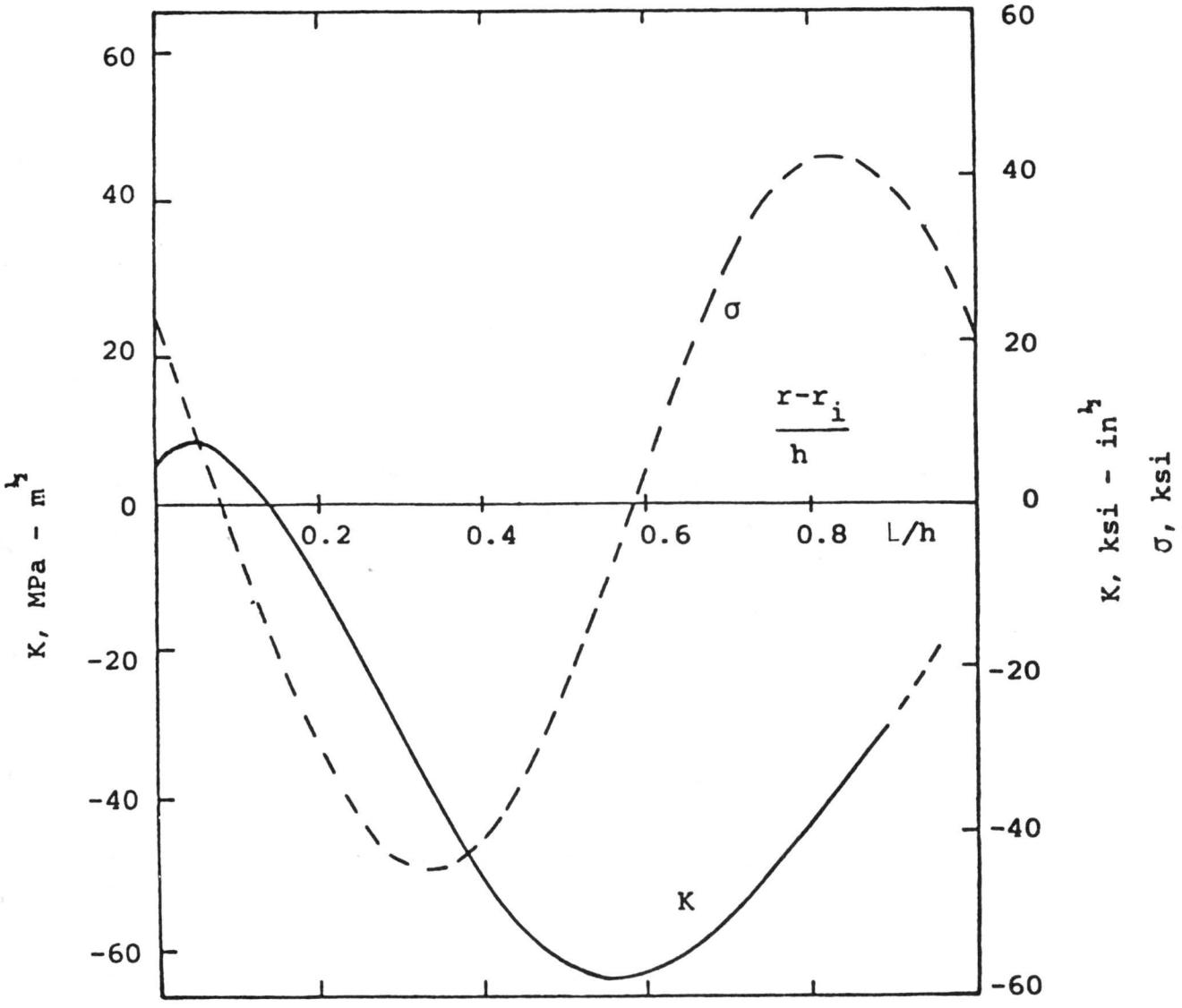

Fig. 6 Residual Axial Stress (dotted curve) and Resulting k-factor (a/b = 0.91).

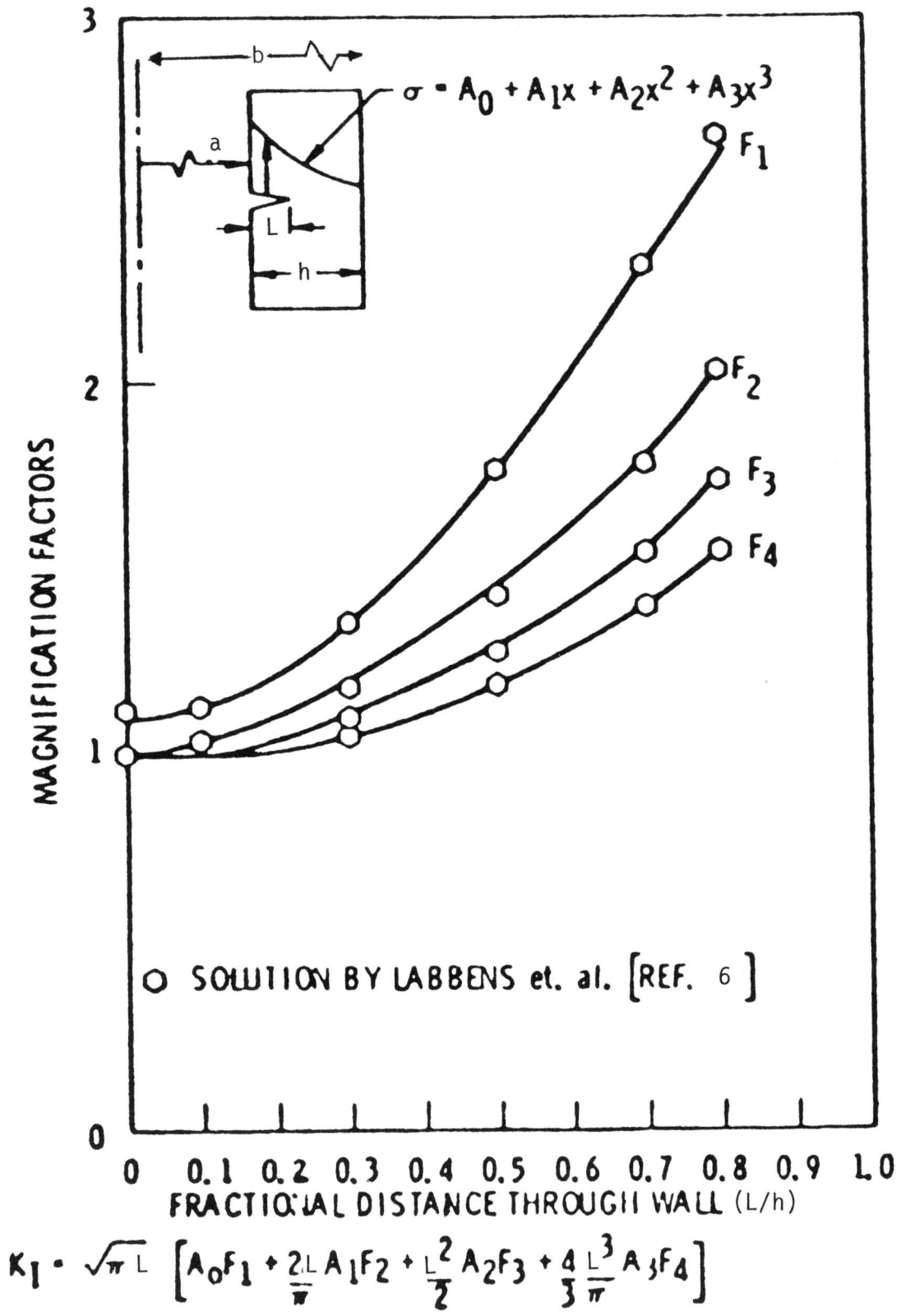

Fig. 7 Magnification Factors for a Circumferential Crack in a Pipe With a/b = 0.91 (Refs. 4 and 9).

Reference [4]. There is a close agreement between the two results and, in case of constant applied stress $(\sigma(X) = A_0)$, with the ones presented earlier. This form of solution can be used to yield good estimates of the k-factors for residual stress patterns that can be approximated by third degree polynomials. The procedure involved is illustrated by considering few typical examples:

Example (1): Consider the residual stress pattern defined in Equation (3) and shown graphically in Figure (6). Employing the method of least square curve fitting, this stress profile can be approximately represented by the cubic polynomial

$$\sigma(X) = 37.63 - 501.80X + 929.40X^2 - 42.00X^3 \quad , \quad (6)$$

The resulting stress intensity factors in a cracked 28" pipe (thickness = 1.384") can be readily computed from equations (4) and (5) and the results are shown in Table (5). In the same table the k-factor, previously given in Figure (6), are also listed to facilitate comparison. The difference between the two results can be attributed to: (1) the poor correlation between the cubic polynomial in Equation (6) and the actual stress variation given by Equation (3), and (2) the nature of the numerical techniques used in both methods. It is clear from Table (5) that the values of the k-factors for the 28" pipe are negative over most of the pipe thickness. Accordingly, the residual k-factors tend to mitigate or even prevent crack growth.

Example (2): An actual through wall residual stress measurement in a 28"-diameter pipe is shown in Figure (8). It was developed by Shack, et al., at Argonne National Laboratory [7] using strain gage measurement techniques. The data was taken at locations 0.31 inch from the weld center line. Employing a polynomial of third degree, the measured stress can be represented by the relation

$$\sigma(X) = 37.79 - 382.3X + 618.7X^2 - 268.6X^3, \ (0 \leq X \leq 1.384) \quad , (7)$$

The resulting stress intensity factors are computed from Equations (4) and (5) and are given in Table (6). As in the previous example, the k-factors assume negative values over most of the pipe thickness.

Table (5): Stress Intensity Factors for Axial Residual Stress - 28" Pipe

$\frac{L}{h}$	K-Factors (ksi$\sqrt{in}$)	
	Cubic stress profile (Eq. 6)	Influence functions (Fig. 6)
0.1	32.27	7.00
0.2	- 16.61	- 12.00
0.3	- 37.85	- 32.50
0.4	- 48.83	- 51.00
0.5	- 53.72	- 62.00
0.6	- 54.26	- 62.50
0.7	- 55.69	- 56.00
0.8	- 54.86	- 42.00

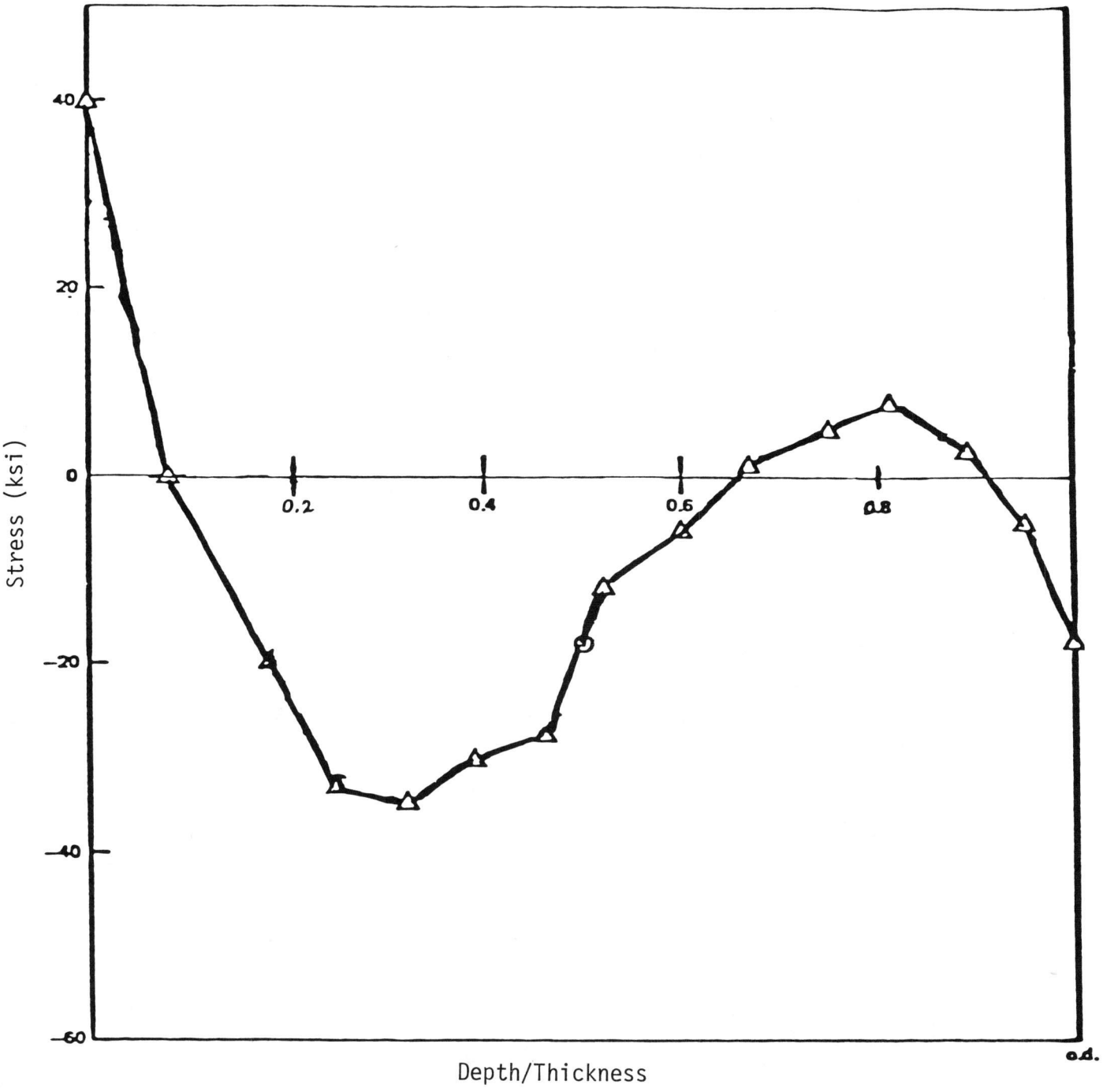

Fig. 8 Through-Wall Residual Stress Measurements on 28-in Diameter Pipe (ANL, Ref. 7).

Table (6): Stress Intensity Factors for Residual Stress Measurements Shown in Figure (8)

L/h	0.1	0.2	0.3	0.4	0.5	0.6	0.7	0.8
k ksi(in)$^{1/2}$	8.79	-5.03	-22.15	-34.54	-44.34	-54.53	-65.06	-80.30

Table (7): Stress Intensity Factors for Axial Residual Stress in Figure (9)

L/h	K-Factors (ksi $\sqrt{in}$)		
	4" pipe	12" pipe	28" pipe
0.1	9.811	15.068	10.211
0.2	13.117	20.140	10.340
0.3	15.413	23.673	- 8.091
0.4	16.845	25.872	- 8.912
0.5	18.049	27.721	- 5.730
0.6	16.682	25.622	- 3.640
0.7	17.507	26.890	- 8.552
0.8	13.279	20.395	-23.923

Example (3): From the survey of the literature [10], typical through-wall residual stress distributions in small and large diameter BWR pipes are as shown in Figure (9). For small diameter pipes (with thickness < 1") the axial residual stress pattern is basically linear with a tensile stress of about 30 ksi on the inside surface and a similar compressive value on the outside surface. For a 4"- diameter pipe (outside diameter = 4.544", thickness = 0.377") the distribution of axial residual is given by

$$\sigma(X) = 30 - 178.042\ X, \quad (0 \leq X \leq 0.377) \quad , \tag{8}$$

and the corresponding values of the k-factors across the pipe thickness are shown in Table (7). Similarily, for a 12"- diameter pipe (outside diameter = 12.5", thickness = 0.795") the residual stress is

$$\sigma(X) = 30 - 75.472\ X, \quad (0 \leq X \leq 0.795) \quad , \tag{9}$$

and the k-factors are computed from Equations (4) and (5) and are shown in Table (7). In contrast to previous examples, the stress intensity factors for smaller diameter pipes are positive over the entire pipe thickness and, therefore, tend to accelerate crack growth. This is in agreement with actual field experience where small diameter BWR pipes are more prone to stress corrosion cracking than large diameter pipes.

For large diameter pipes (with thickness > 1"), the k-factors corresponding to the residual stress pattern shown in Figure (9) are also computed and the values are listed in Table (7). For this case also, the values are negative over most of the pipe thickness as in previous examples.

Example (4): As a final example, consider the distribution of axial residual stress in the vicinity of a full circumferential weld shown in Figure 10. This distribution was utilized in Reference [11] to predict the behavior of stress corrosion cracking in large diameters BWR piping. For a 28" pipe with thickness X = 1.384", the residual stress can be represented by the equation

$$\sigma(X) = 29.967 - 166.846X + 191.67X^2 - 59.558X^3 \quad , \tag{10}$$

Wall Thickness	Through-Wall Residual Stress	
	Axial	Circumferential*
0 to 1 inch	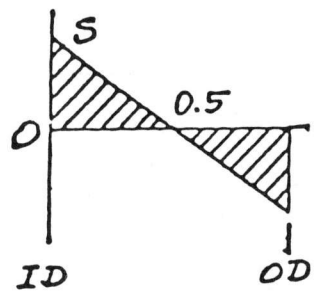	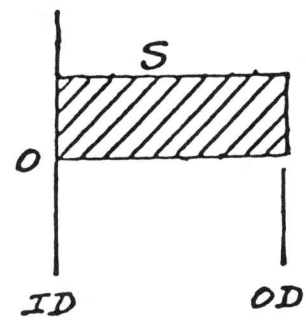
> 1 inch	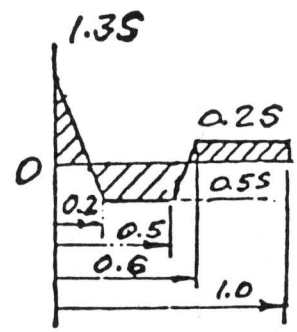	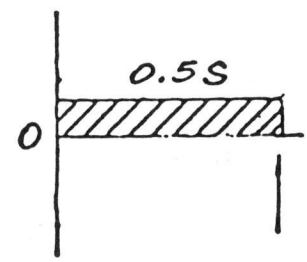

Fig. 9 Typical Distribution of Through-Wall Weld Residual Stress (S = 30 ksi).
*Considerable Variation With Weld Heat Input.

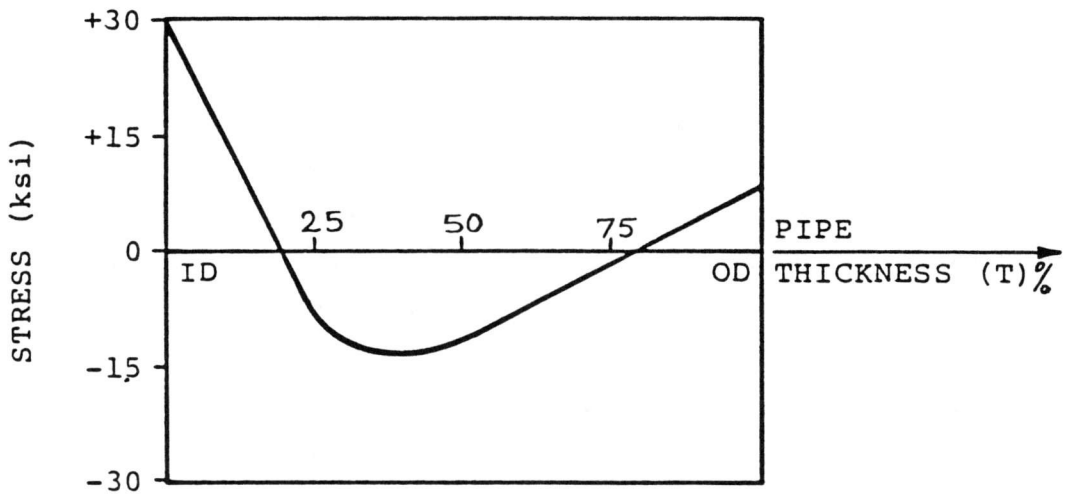

Fig. 10 Axial Residual Stress Distribution (pipe diameter of 20 to 28 in, Ref. 11).

and the resulting stress-intensity factors are given in Table (8). As can be seen from the table the k-factor for this case becomes negative at an L/h value close to 0.4.

B. Long Axial Cracks:

Since the elasticity problem of a cylinder containing a part-through axial crack appears to be analytically intractable, numerical techniques such as the boundary integral equation [4,12] and finite element methods [9,13-15] have been employed to estimate the stress-intensity factors for such cases. In this section, the stress magnification at the tip of a long axial crack is given. The geometry of a long axial crack in a cylinder is shown in Figure (11). L denotes the crack depth and x is a variable parameter across the thickness of the pipe. Stress intensity solutions based on integration of the proper influence functions in the boundary integral equation method are available in the work cited by Labbens, et al. [4] and by finite element method in the work of Buchalet and Bamford [9]. The solutions are applicable to pipes with a/h = 10 (i.e., a/b = 0.91) and arbitrary crack depths. For polynomial loading across the crack surfaces which can be represented by the relation given in Equation (4), the stress intensity factor is obtained from the formula previously described in Equation 5. For this case, however, the magnification factors F_1 , .., F_4 are as shown in Figure (12). The dotted curves are based on work described in Reference [9], while the solid curves are based on work given in Reference [4]. As can be seen from the figure, there is a close agreement between the two results especially for shallow crack depths.

The stress intensity factors for long axial cracks in pipes (with a/h = 10) can also be obtained using the computer code described in Reference [8]. These solutions are accurate to within 5% for L/h (crack depth to pipe wall thickness ratio) less than 0.9. Instructions on how to use the computer code and further details are available in Reference [8].

C. Semi-Elliptical Part-Through Axial and Circumferential Cracks

Interior axial cracks in pressure vessels usually form at the surface in the weld heat-affected zone, and since this zone is limited to about 1/4" on either side of the weld, these cracks remain very short in the axial direction

Table (8): Stress Intensity Factors for Residual Stress Shown in Figure (10) - 28" Pipe

$\frac{L}{h}$	L (in.)	K-Factors (ksi $\sqrt{in}$)
0.1	0.1384	13.515
0.2	0.2768	10.835
0.3	0.4152	5.033
0.4	0.5536	- 0.861
0.5	0.692	- 6.429
0.6	0.8304	- 14.798
0.7	0.9688	- 19.395
0.8	1.1072	- 29.908

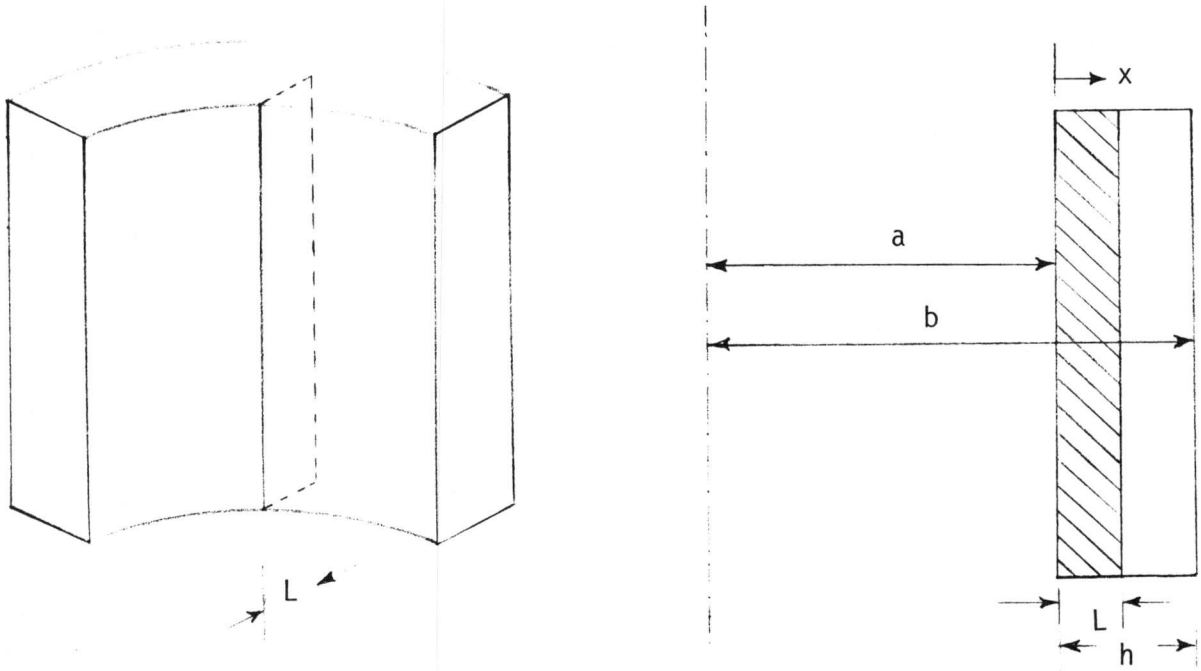

Fig. 11 Geometry of Long Axial Cracks in Pipes.

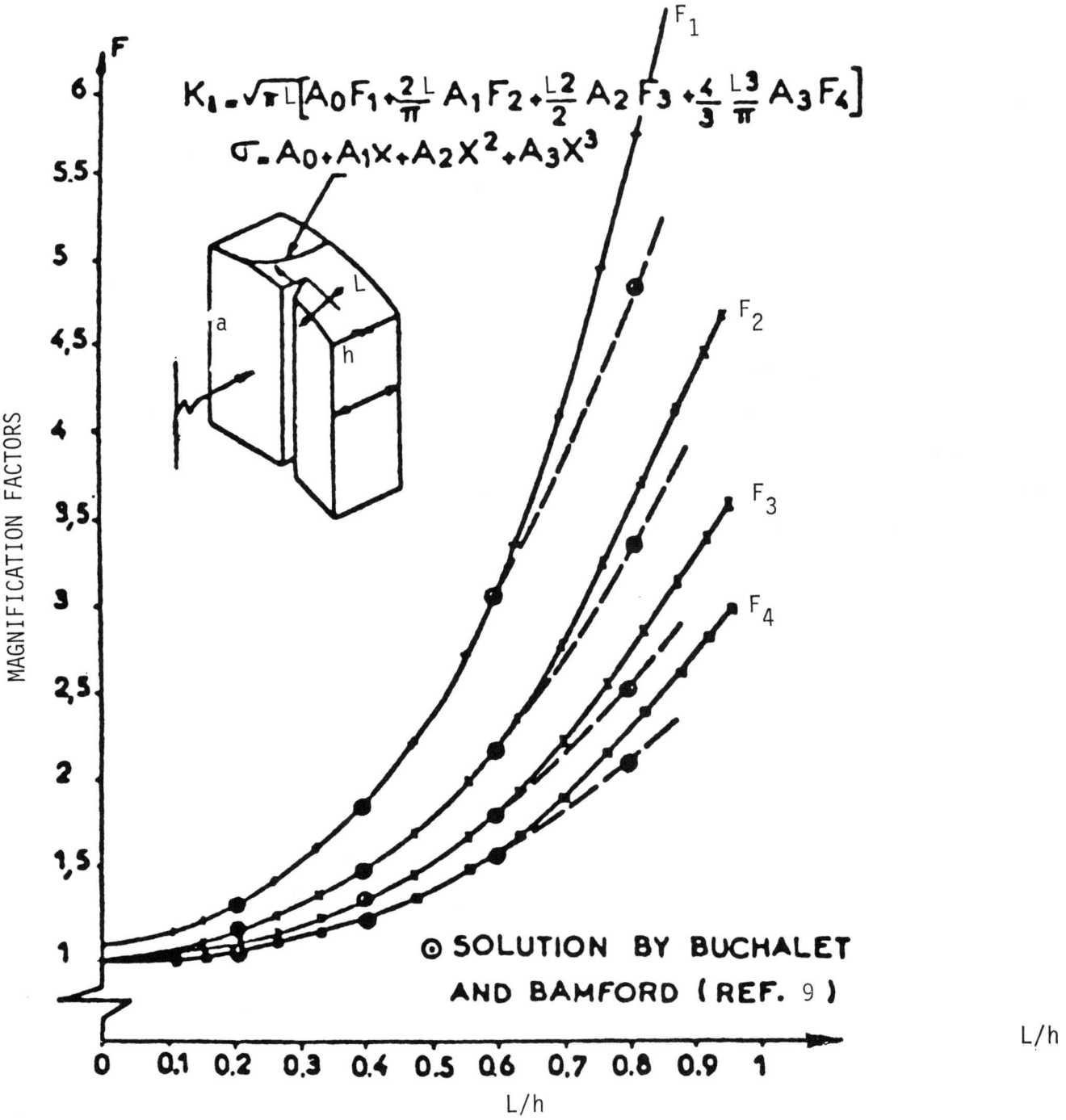

Fig. 12 Magnification Factors for Part-Through Axial Cracks (a/L = 10).

and tend to grow through the wall of the pipe. Similarly, the part-circumferential surface crack is a two-dimensional flaw or a plane of discontinuity that requires two length dimensions for its specifications. Both these cracks can be conveniently modeled by a semi-elliptical shape, and by varying the axes of the ellipse, several practical shapes of interior surface cracks can be covered. Stress-intensity factors for such flaws have been obtained numerically using boundary integral equation approach [12] and finite elements methods [14,15] and experimentally by photo-elastic methods [16]. Some of these results are presented in this section.

Semi-Elliptical Axial Flaw

A longitudinal semi-elliptical crack is one of the common flaw types to be found in pressure vessels. Figure (13) shows the geometry of such a flaw. The semi-major and semi-minor axes of the ellipse are denoted by c and L respectively. The ASME Boiler and Pressure Vessel Code recommends a flaw with c/L = 3 in a cylinder with an outer to inner radius ratio of 1.1. For such cracks the stress intensity factor varies along the crack border (i.e., it is a function of the parameter ϕ defined in Figure (13). For crack surface loading described by the expression

$$\sigma(x) = A_o + A_1\left(\frac{x}{h}\right) + A_2\left(\frac{x}{h}\right)^2 + A_3\left(\frac{x}{h}\right)^3, \tag{11}$$

where $A_o, \ldots A_3$ are specified constants, the stress intensity factor is given by the relation [14]

$$k(\phi) = \left(A_oH_o + \frac{2L}{\pi h}A_1H_1 + \frac{L^2}{2h^2}A_2H_2 + \frac{4L^3}{3\pi h^3}A_3H_3\right) \cdot \left(\frac{\pi L}{Q}\right)^{1/2} \cdot \left(\cos^2\phi + \frac{L^2}{c^2}\sin^2\phi\right)^{1/4} \tag{12}$$

in which

$$Q^{1/2} = \int_o^{\pi/2} \left[\cos^2\phi + \left(\frac{L}{c}\right)^2 \sin^2\phi\right]^{1/4} d\phi \tag{13}$$

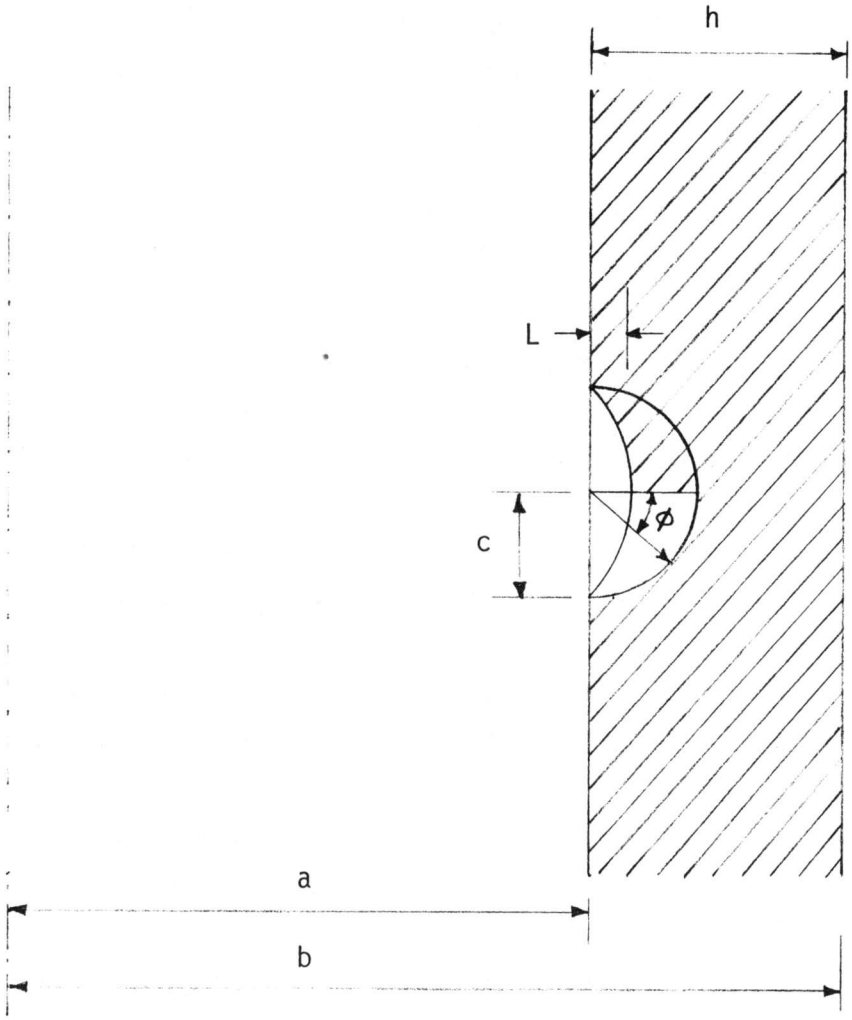

Fig. 13 Geometry of Semi-elliptical Longitudinal Crack.

and H_0, H_1 H_2 and H_3 are magnification factors which vary with the parametric angle (ϕ) of the flaw. They are displayed graphically in figures (14 through 16) for crack depths L/h = 0.25, 0.5 and 0.8, respectively. Except for H_0, the magnification factors are maximum at the point of greatest depth in the wall ($\phi = 0$). In the three cases discussed, H_0 has maximum at $\phi = \pi/2$, i.e., at the intersection of the crack with the free surfaces. Reference [14], also compare these results with those obtained in References [12] and [15] for identical geometries and constant loading. Generally speaking all three results agree within 10% range especially for low values of ϕ. For large values of ϕ there is a more significant difference between the three results. The interested reader should refer to [14] for further details.

Semi-Elliptical Circumferential Planar Flaw

The geometry of a semi-elliptical circumferential flaw near the interior surface of a pipe is shown in Figure (17). The crack depth is defined by L and C represents the half surface length. Reference [8] describes a numerical procedure (and a computer code) based on the influence functions of Reference [4] to derive root-mean-square average stress intensity factors for this flaw under arbitrary stress symmetrical across the minor axis of the semi-elliptical crack. Furthermore, by comparing the results for part-circumferential and longitudinal semi-elliptical cracks, these authors reach the conclusion that the values for these two cases do not differ widely. Therefore, the longitudinal results should provide reasonable approximation to the circumferential cracks under similar loading. It seems that there is room to refine the calculation of Reference [8] for this type of flaw to achieve better accuracy in the results and the authors of Reference [8] indicate that they are working at this matter.

III. EXPERIMENTAL CRACK GROWTH RATES

This section deals with the analysis of available experimental data on the growth behavior of cracks in austenitic stainless steel of the type used in nuclear power plants. Laboratory data generated by various organizations

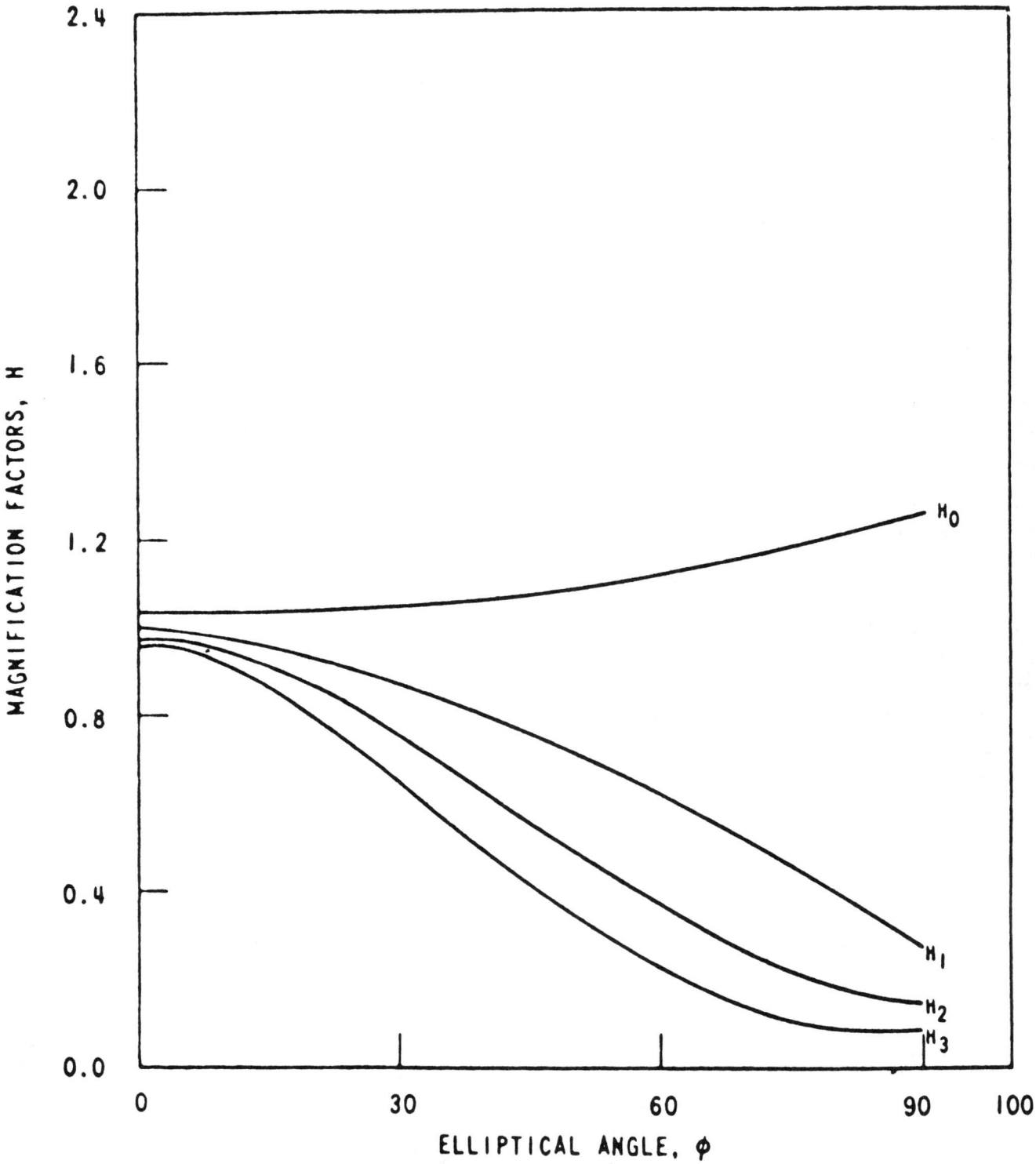

Fig. 14 Magnification Factors for a Semi-elliptical Longitudinal Flaw in a Pipe (a/b = 0.91, L/h = 0.25, c/L = 3).

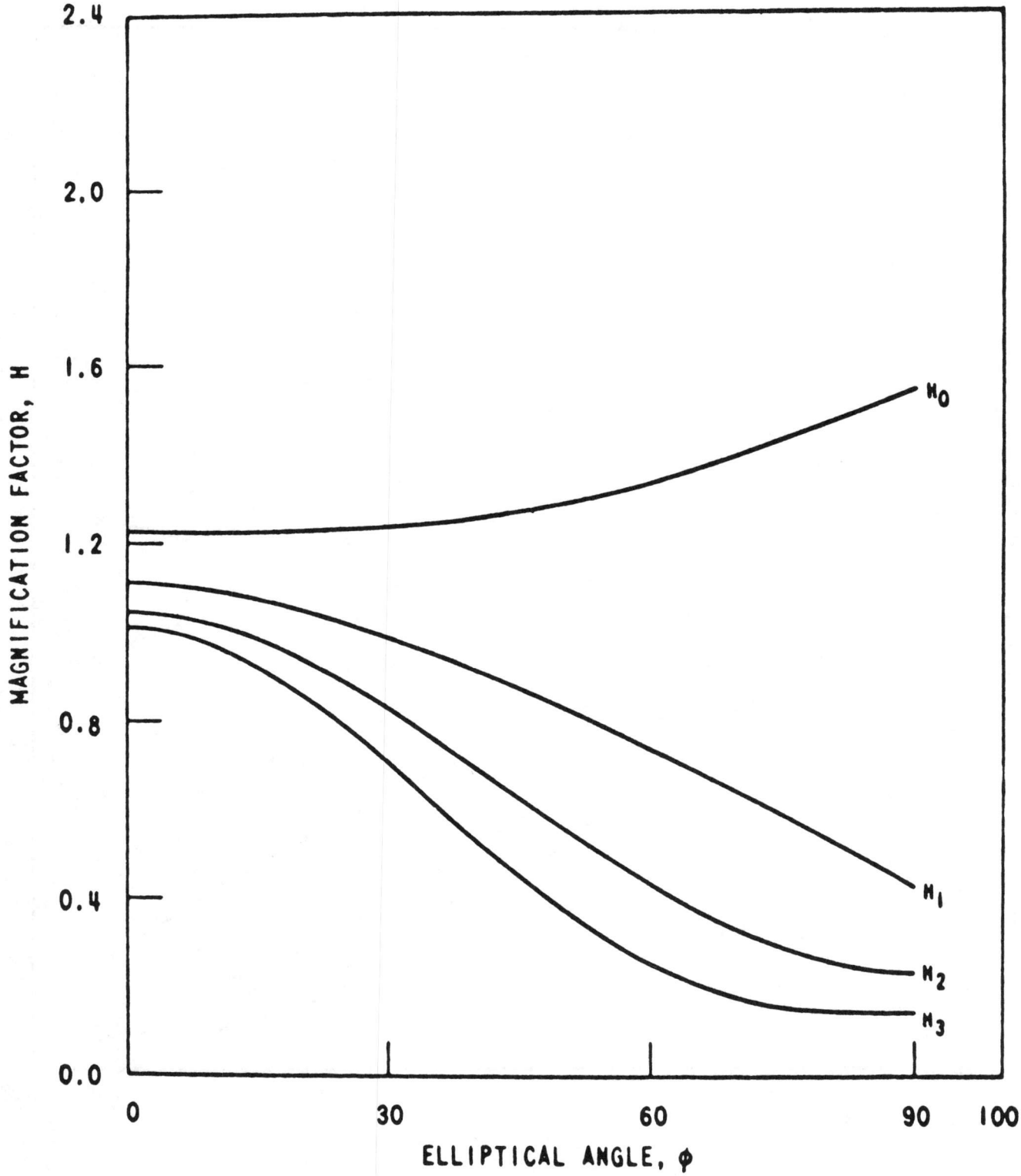

Fig. 15 Magnification Factors for a Semi-elliptical Longitudinal Flaw in a Pipe (a/b = 0.91, L/h = 0.50, c/L = 3).

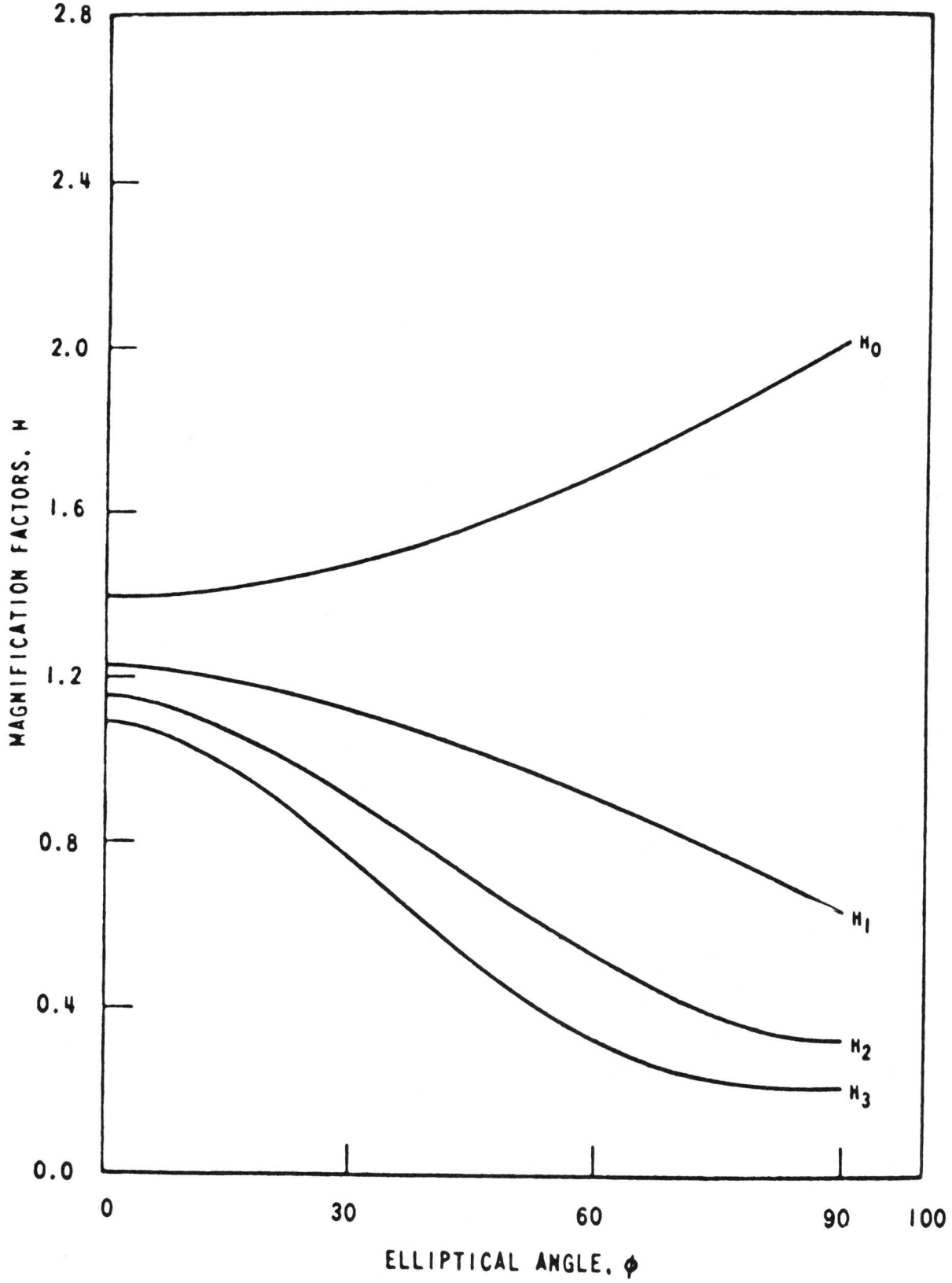

Fig. 16 Magnification Factors for a Semi-elliptical Longitudinal Flaw in a Pipe (a/b = 0.91, L/h = 0.8, c/L = 3).

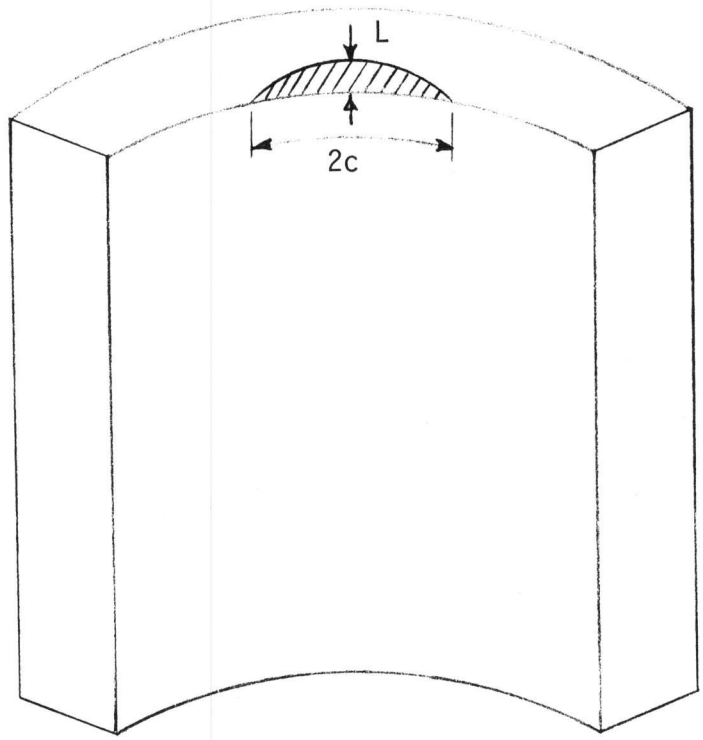

Fig. 17 Semi-elliptical Part-through Circumferential Crack.

are examined in order to develop realistic curves to evaluate crack growth rates for detected flaws in BWR piping systems. The curves can be used to derive mathematical expressions relating the crack extension rate as a function of the applied stress intensity factor. Thus, by employing the proper values of the stress intensity factors for various loading conditions, a time estimate can be made for an initially detected flaw to reach the allowable size. Examples to illustrate the application of the aforementioned curves to predict the growth behavior of typical flaws in BWR piping systems are provided in Section IV of this report.

Stress corrosion crack growth rates are usually measured in the laboratory as functions of the applied stress intensity factors. The standard tests performed include the cantilever bend test and the constant displacement bolt-loaded compact tension test. Test results show that the magnitude of the growth rate is influenced by the three main factors discussed below:

(1) Mode of Applied Loading:

The applied loading on the specimen can be either constant or cyclic. Constant loadings produce stress corrosion growth while periodic loadings are associated with corrosion fatigue growth. Due to the additional mechanical component of fatigue, cyclic loading causes higher crack growth rate than that obtained for non-cyclic loading. During normal operation, a typical pipe in a nuclear power plant experiences both static and transient loadings. The constant or static loadings consists of internal pressure, dead weight and welding residual stresses, whereas the transient loadings are due to the thermal transient conditions which cause differential thermal expansions. From the initial review of the literature it seems that the resulting periodic stresses are not significant and thus the assumption is made that the affected area (weld joint) sustains constant loading during the design life of the plant and that any fatigue can be neglected.

(2) Environment (Water Chemistry and Temperature):

It is known that the concentration of dissolved oxygen as well as some diluted levels of sulfates and chlorides in the environment affect the growth of corrosion cracking in the pipe. For the dissolved oxygen, the mode of

loading has a strong influence on the growth rate. In tests conducted under constant loading, the rate of crack growth increases with the increase of O_2 concentration from 0.2 to about 5 ppm, while at higher concentration (up to 8 ppm) crack growth rate remains almost constant. In slow strain tests, the corrosion potential and crack growth rate is higher at the 8 ppm level than the 0.2 ppm level. As far as the sulfates and chlorides are concerned, a level of about 1/10th ppm in both HCL and H_2SO_4 can accelerate IGSCC in slow strain experiments.

Since under normal operating conditions of boiling water reactors, the environment includes a temperature of about 288°C (550°F) and a concentration of coolant O_2 of about 0.2 ppm and some dilute solutions of electrolytes that are within the Regulatory Guide limits on conductivity,only the results of experiments performed within these specifications will be reviewed in the report.

(3) Degree of Sensitization

The available experimental data gives a clear indication that the most important factor affecting the crack growth rate is the level of sensitization present in the material in the heat affected zone near the weld joints where intergranual cracks are usually situated. Faster crack growth (almost by an order of magnitude) can be achieved by applying a high degree of sensitization to the same specimen assuming all other factors are identical. Sensitization dependes on the sensitizing heat treatment and on the material carbon content. An electrochemical method utilizing the so-called EPR values (Electro-chemical Potentiokinetic Reactivation) has been developed to detect and measure the degree of sensitization. EPR values of up to 10 C/Cm^2 indicate low levels of sensitization while values in the range (20-30) C/Cm^2 correspond to high degree of sensitization. It has been suggested that an isothermal treatment of a test specimen for 2 hours at $\backsim$ 600°C (1150°F) gives rise to low levels of sensitization (EPR = 10 C/Cm^2), whereas heat imparted to the specimen at $\backsim$ 600°C (1150°F) for (8-24) hours results in a high degree of sensitization (EPR = (20-30) C/Cm^2). Of course, the relevant heat treatment given to laboratory specimens must be such as to impart a level of sensitization resembling that produced in the pipe heat-affected zone during the

welding process. In existing BWR installations it is difficult to estimate the degree of sensitization in the weld joints since, as mentioned, it is influenced by numerous factors. Moreover, there is experimental evidence which shows that the presence of chromium carbides along the grain boundaries can cause sensitization of type 304 stainless steel at temperatures well below the required normal isothermal sensitization range [17,18]. All that is needed is sufficient heat treatment capable of forming chromium carbides nuclei. This suggests that the degree of sensitization in the weld joints of an operating BWR pipe can increase with time and result in accelerated cracking. For these reasons, it is prudent to explore crack growth rates generated from specimens subjected to various levels of possible sensitization in order to arrive at rational evaluation curves.

Experimental Data

Reference [19] presents a survey of crack growth rates for type 304 stainless steel in high purity water under stress corrosion cracking. Data from eleven series of laboratory tests, conducted by various organizations throughout the world in the late seventies were compiled and analyzed to determine the important parameters and their influence on the rate of crack growth. These parameters include mode of applied loading, concentration of dissolved oxygen and degree of sensitization. The results obtained from experiments performed under constant loading, and environment similar to those found in typical operating BWR plants were collected and displayed graphically. Essentially, these were taken from the results published by Ford and Silverman [20], and Horn, et al. [21]. Ford's data were obtained from tests performed in high purity water at 95°C, with 1.5 ppm oxygen. The specimens had a carbon content of 0.065% and were sensitized at 600°C for 24 hours. The aim of the study was to assess the influence of loading frequency, which varied from 3×10^{-5} Hz to 6 Hz, and mean stress on the crack growth. Horn's data, on the other hand, were obtained from specimens in water at 288°C with 0.2 ppm of dissolved oxygen. These were only subjected to static loading. The degree of sensitization was measured by the electrochemical potentiokinetic reactivation (EPR) method with EPR values varying between (13-27) C/CM^2.

The overall trend of the results is fairly linear on a log-log plot depicting of crack growth rates vs. stress intensity factors. Using the equation of a straight line, a mathematical expression can be derived to represent the crack growth rate as a power function of the k-factor. Reference [19] gives the following relation which represents the best estimate of crack growth rates;

$$\frac{dL}{dt} = 1.843 \times 10^{-12} k^{4.615}, \tag{14}$$

Upper and lower bound estimates are also given. For the upper bound estimate, the equation of the crack growth is:

$$\frac{dL}{dt} = 4.116 \times 10^{-12} k^{4.615}, \tag{15}$$

while for the lower bound, the corresponding relation is

$$\frac{dL}{dt} = 0.766 \times 10^{-12} k^{4.615}, \tag{16}$$

Besides the above described work other published as well as unpublished results of work currently in progress have been examined. Specifically, Reference [22] contains the results of a comprehensive experimental program carried out by the General Electric Co. (Nuclear Engineering Division) over a 4-year period (1978-1982) to evaluate the behavior of stress corrosion cracking in large diameter type 304 stainless steel pipes. Some of the results of this program (see e.g., the work of Horn, et al. [21]) have been incorporated in Reference [19] to arrive at Equation (15) used for an upper bound growth curve. In order to assess the effects of the environment on crack growth, the data generated by experiments depicting the in-service conditions of the piping component was evaluated. From these results it was observed that the level of sensitization is the most critical factor controlling crack growth rates. Two schemes of laboratory sensitizations have been employed:

(1) A heat treatment of 1150°F (621°C) for 2 hours to impart a low level of sensitization to the speciment (EPR $\sim$ 10 C/CM^2) and (2) A furnance sensitization of the same amount of heat for 24 hours to yield a severe level of sensitization (EPR $\sim$ 30 C/CM^2).

Two crack growth evaluation curves are generated from the data of the test program in Reference [22], and these are exhibited in Figure (18). In the same figure, additional constant loading data generated by other organizations, are also given for comparative purposes. The source of the additional data is stated in the legend of Figure (18). The top curve represents an upper bound in the sense that it encloses all data points plotted. It can be used when the degree of sensitization is known to be high. This curve represents data points obtained from experiments conducted in 0.2 ppm oxygenated water and also in water with 8 ppm oxygen (which is known to be more aggressive). These results clearly substantiate the observation mentioned earlier that the sensitization level outweighs the effect of oxygen concentration on the rate of crack growth. The lower curve represents data measured from specimens subjected to lower levels of sensitization. Its shape displays typical stress corrosion behavior, namely, three-stage development with a plateau region in the middle indicating appreciable loading without any crack movement. Examination of the location of the majority of data points in Figure (18) clearly confirm that "The lower representative curve is not as strongly supported by the data as is the upper bound curve" as stated in Reference [22]. The lower curve, however, has been suggested [22] to explain field expereience. Figure (19) shows the aforementioned two curves with the relevant points predicted by Equation (15). Clearly, Equation (15) predicts behavior similar to the lower curve.

Recent data on crack propagation rates obtained from Argonne National Laboratory [23, 24] was also examined. Some of this data is shown in Figure (20) along with the two evaluation curves mentioned previously. The ANL data was generated in high purity water containing 8 ppm dissolved oxygen. The specimens were sensitized by subjecting them to 1292°F heat treatment for periods varying from 10 minutes to 14 hours resulting in EPR values ranging from 4 C/CM^2 to 15 C/CM^2, respectfully. As shown in Figure (20), the ANL data lie between the two curves of Reference [22].

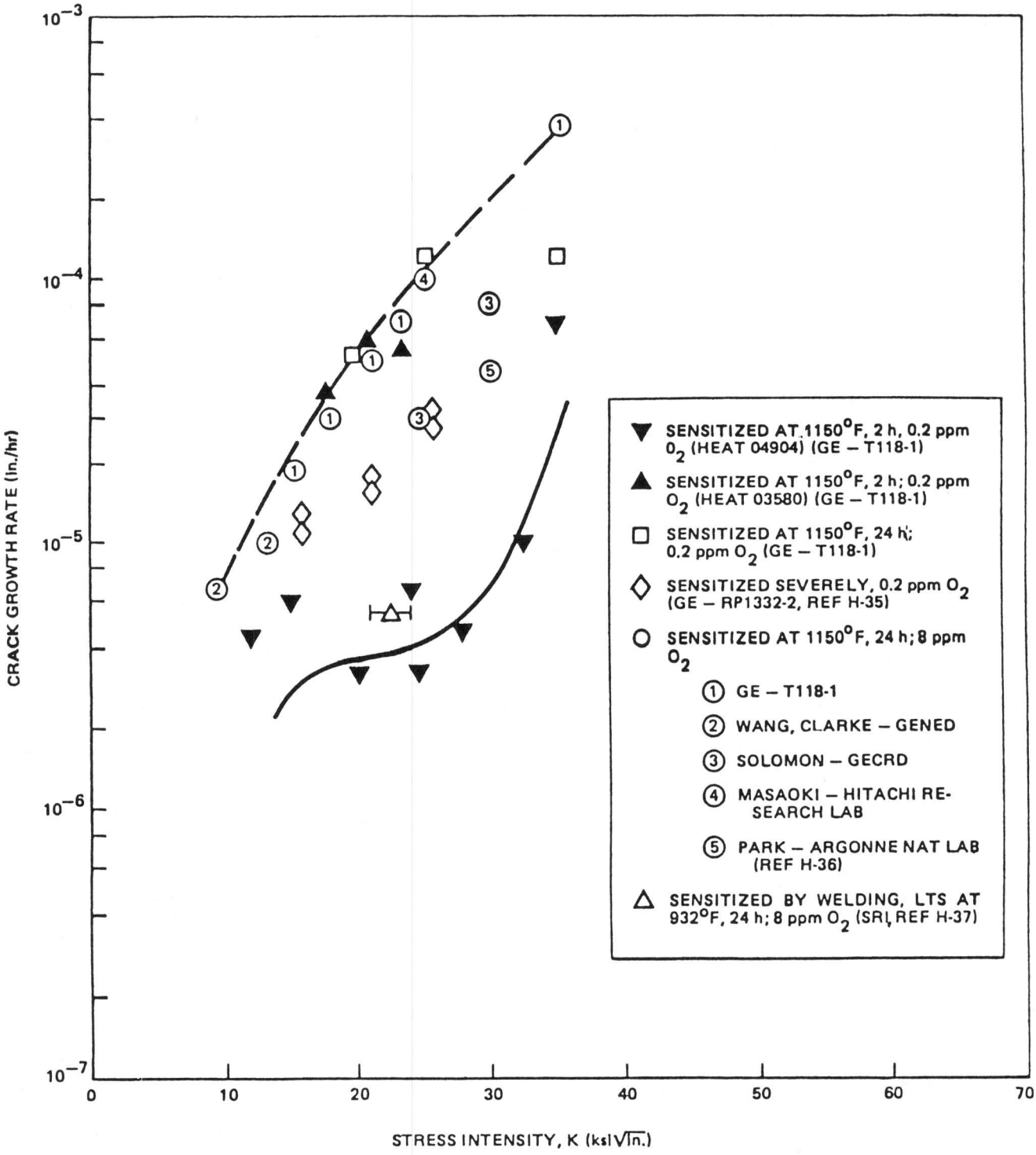

Fig. 18 Summary of Constant Load Crack Growth Data (Curves are evaluation curves). Data collected in 0.2 ppm O_2 and 8 ppm O_2 water. Different levels of sensitization examined.

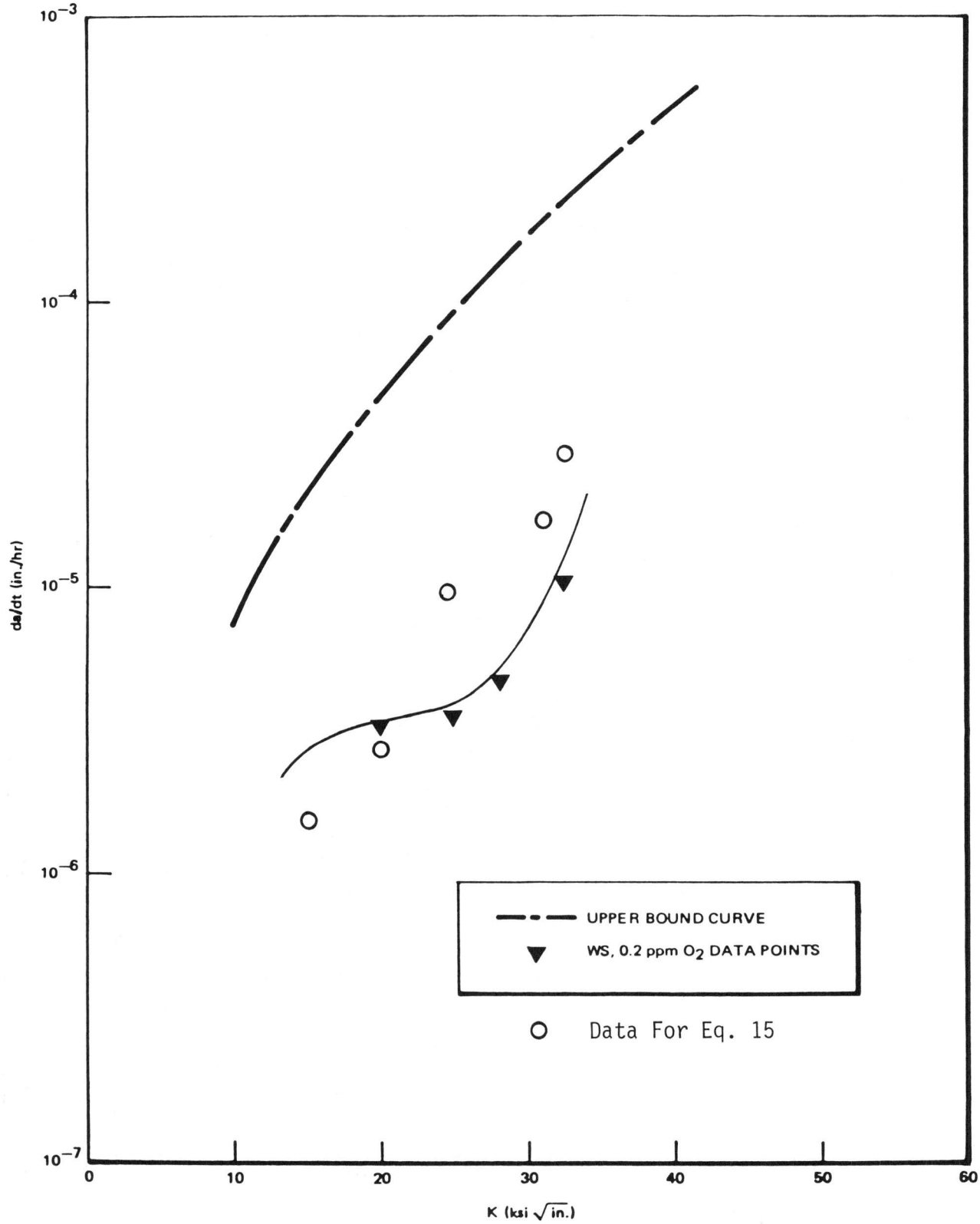

Fig. 19 Constant Load Crack Growth Rates Measured as a Function of Stress Intensity Factors.

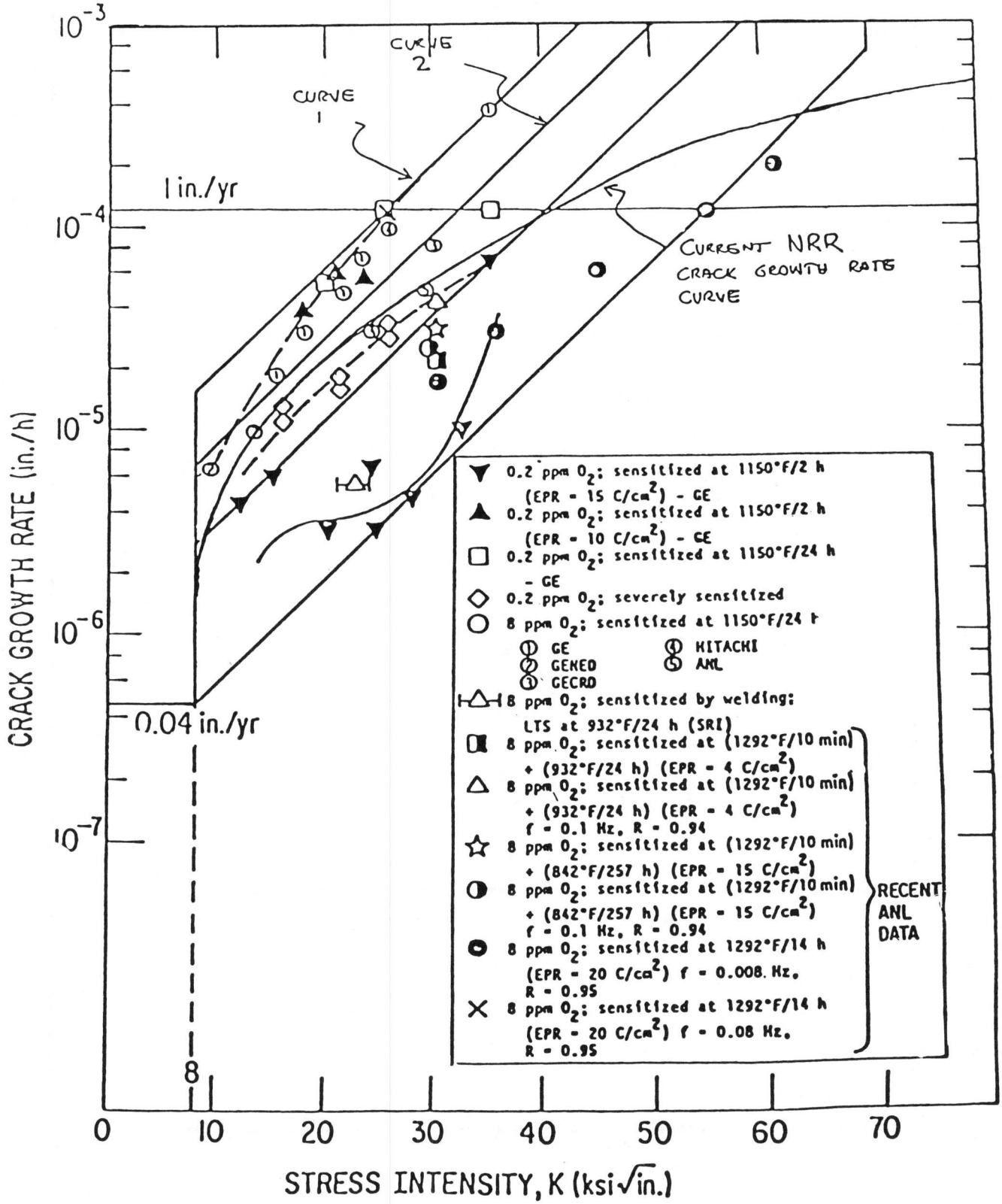

Fig. 20 Crack Growth Rates vs. Stress Intensity Factors (ANL,23).

Additional experiments currently in progress at ANL indicate that the presence of impurities (such as sulfates and chlorides) in the environment could influence the crack growth rate [24]. The levels of impurities included in the investigation are within the Regultory Guide limits on conductivity. ANL scientists estimate that in slow strain rate tests, an addition of 1/10th ppm of sulfate as H_2SO_4 to the environment will increase the crack growth rate by a factor of 3. Their initial results indicate that in the presence of such impurities, cracks in slightly sensitized specimens subjected to static or slow strain loading propagate at faster rates than the furnace sensitized materials. This observation has been confirmed with both CERT (constant extension rate tests) and compliance experiments. This, of course, is not true in pure water. But, it could explain some of the accelerated crack growth observed in the field. The experiments at ANL also indicate that the addition of hydrogen will render the material more tolerant to impurities. Since this work is currently in progress and the results are incomplete, the effects of impurities on crack propagation rates cannot be assessed completely, especially in a quantitative manner. Generally, however, dilute levels of impurities seem to be another source that would accelerate stress corrosion cracking in BWR piping systems.

Crack Growth Law

In order to determine mathematical expressions for the rate of crack growth under normal operating conditions, the data points of the two bounding curves shown in Figure (18) are plotted on a log-log scale as shown in Figure (21). As expected, the data indicates linear variation between the crack growth rate (in./hour) and the k-factor (ksi$\sqrt{\text{in}}$). The data from the lower band (curve 1) yield the formula

$$\frac{dL}{dt} = 2.258 \times 10^{-9} \quad K^{2.429},$$

and for the data in the upper band, the best estimate corresponding to the dotted line (curve 3) is described by the relation

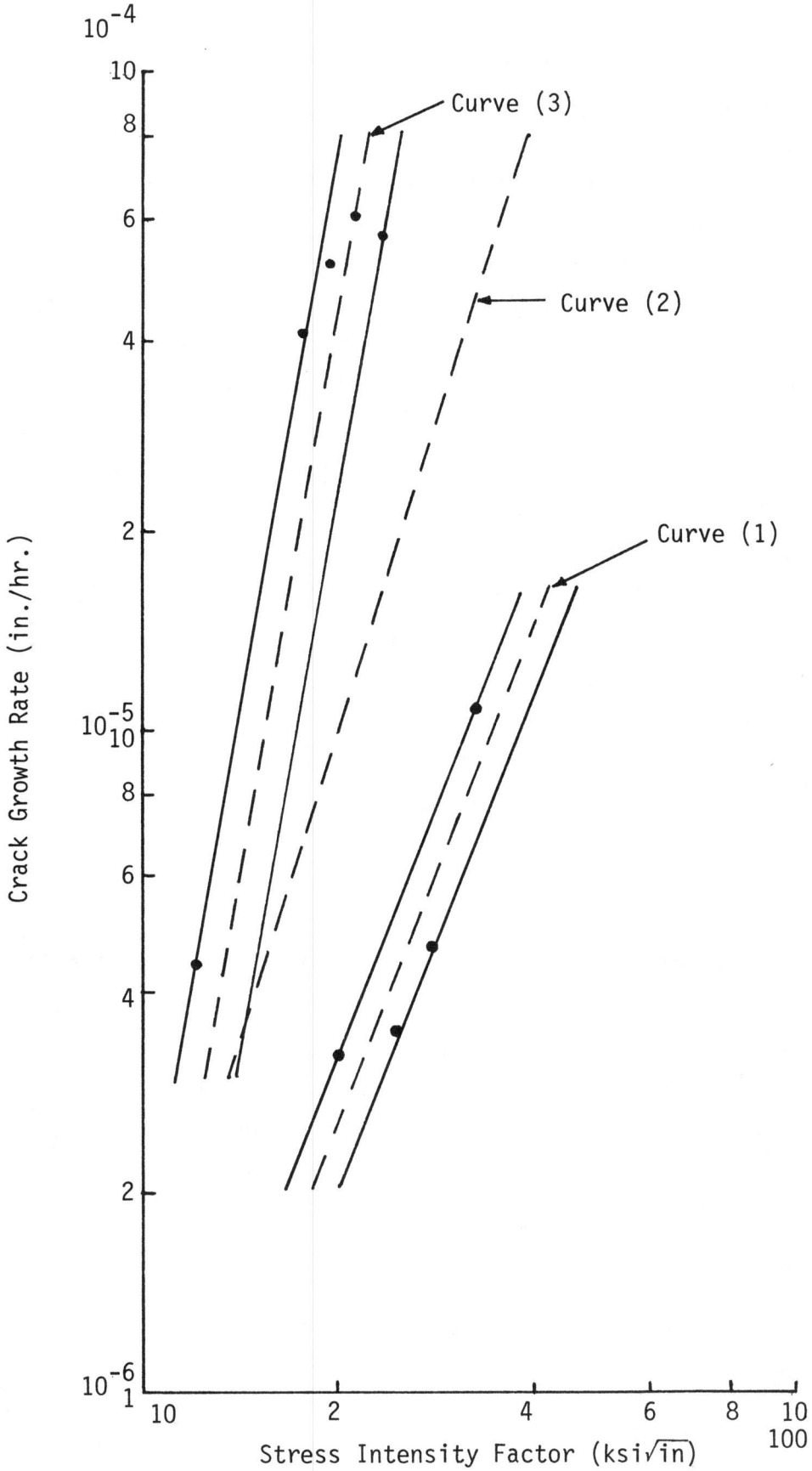

Fig. 21 Crack Growth Rate of Sensitized 304 Steel.

$$\frac{dL}{dt} = 2.241 \times 10^{-12} K^{5.40}, \qquad (18)$$

Additional data points from Figure (20) are also plotted in Figure (21) and indicated by curve 2. These experimental results fall between the two extreme bands mentioned previously. The corresponding crack growth law is represented by the formula

$$\frac{dL}{dt} = 9.55 \times 10^{-10} K^{3.09}; \qquad (19)$$

These crack growth laws will be used in Section IV of this report to compute and compare the time required for certain hypothetical flaws in large and small diameter BWR pipes to reach the corresponding code allowable size. A parametric study utilizing the various crack growth formulas in conjunction with the relevant k-factors for applied and residual stresses is performed to assess the time interval required to undertake routine inspection of the piping system.

IV. EVALUATION OF CRACK GROWTH IN WELDED BWR PIPING SYSTEM

According to the ASME Boiler and Pressure Vessel Code [25], the allowable depth of a crack in a BWR pipe can be conservatively calculated by adopting the specific procedure recommended by the code for critical crack size. For subcritical crack growth, it is necessary to compute the total crack growth that will occur over a given period of time in order to find out how long it will take to reach the allowable depth. Moreover, the incubation time of the crack plays an important role in decisions effecting continued service of the system, and in the planning of in-service inspection periods. Crack growth due to both fatigue and stress corrosion must be computed and combined in order to assess the available margin to failure.

In this section, hypothetical cracks in BWR pipes are considered to illustrate the use of the k-factors and growth formulas presented above, and to predict the times required for each of the cracks to propagate to allowable depths. A parametric study is performed in order to ascertain the relative importance of the various input factors (residual stress, crack growth law, etc.) which influence the growth behavior of stress corrosion cracks. Cracks in large diameter as well as in small diameter pipes are considered.

Large-Diameter BWR Pipes

Consider a 28-inch diameter recirculation pipe subjected to BWR environment of high purity water at 288°C and a concentration of dissolved oxygen of 0.2 ppm. The outer radius (R) is 14 inches and the thickness (h) is 1.384 inches. A typical stress report for this type of installation written by G.E. Company [26] gives an operating pressure (p) = 1450 psi, and a bending moment due to dead weight and seismic OBE, (M) = 448,920 inch-pounds. It follows that the primary axial stress which consist of membrane (P_m) and bending (P_b) is given by

$$P_m + P_b = \frac{PR}{2h} + \frac{M}{Z} = 7945 \text{ psi}, \tag{20}$$

The thermal expansion stress can be assumed to be about 4055 psi, making a total applied stress of 12 ksi in the axial direction.

Suppose that a 360° circumferential crack with an initial depth of 20% of the pipe wall thickness is detected in the pipe. In order to determine the depth allowed by the ASME Code [25], the stress ratio is computed

$$\text{stress ratio} = \frac{P_m + P_b}{S_m} = \frac{794.5}{16,800} = 0.47; \tag{21}$$

Hence, according to Reference [25], the allowable depth should not exceed 63% of the pipe thickness. In Equation (21), S_m (=16,800 psi) is the code allowable stress, and has a value equivalent to about 1/3 of the flow stress of the material. To find out how long it will take for the crack to propagate to its allowable depth, a crack growth analysis is carried out. The stress intensity factors due to the normal operating stress (12 ksi) are computed at various crack depths of the pipe by using the tables and charts provided in Section I, and the results are given in Table (9). Next, the k-factors due to the weld residual stresses are superimposed on those due to the applied stress in order to obtain the total k-factors or the crack driving forces (see Table 9). The time needed for the crack to propagate can then be computed by using the crack growth laws presented in Section III of this report. Since there are several possibilities of residual stresses and crack growth formulas, the resulting cases will be discussed separately in the sequel.

Case (A): Consider the residual stress distribution shown in Figure (10) which is used by some utilities to predict the behavior of IGSCC. The corresponding k-factors are available in Table (8). Superimposing these values on the k-factors due to the applied stress, the total k-factors on the crack driving forces at various depths across the pipe thickness are obtained as shown in Table (9).

Since fatigue crack growth is negligible, the time required for the crack to propagate from a 20% depth to the allowable depth (63%) is obtained by integrating the growth equations numerically. This can be done most conveniently by a computer program that perform the numerical integration over small intervals of the crack trajectory. Making use of the growth rates presented in Section III, the time predicted for the hypothetical crack to reach its code allowable depth is shown in Figure (22). Note that using the most conservative growth rate, given in equation (18), a time of about 11 months is required for the propagation. Growth rate represented by curve (2) yields about 40 months while the slowest equation represented by growth curve (1) and equation (17) gives a time of 140 months. It is clear that there is a difference of more than an order of magnitude between the use of the most conservative and slowest growth formulas. The time required to propagate form an initial crack size of depth/thickness ratio = 0.1 is also shown in Figure (22) by dotted lines. Basically, the same conclusion holds.

Case (B): A typical through-wall residual stress distribution in large diameter BWR pipes is shown in Figure (9) and the corresponding stress intensity factors are listed in Table (7). Making use of these values, the total stress intensity factors for the applied and residual stresses are given in Table (9). Utilizing the growth rates presented in Section III, the time required for hypothetical cracks (with L/h = 10% and 20%) to reach the code allowable size is displayed in Figure (23). It is clear that in this case a slower crack movement is predicted. This is mainly due to the low values of the operating stress intensity factors in the middle of the pipe wall which in turn are affected by the negative residual stress values. The upper conservative curve (Curve 3) predicts an incubation time of about 50 months for a crack to propagate from a 10% depth to 40% depth and, then, in a mater of a few months, the crack rapidly propagates to the allowable size. The shape of the curves

Table 9. Total Stress Intensity Factors in Large Diameter BWR Pipes (28" Diameter) - ksi$\sqrt{in.}$

L/h	0.1	0.2	0.3	0.4	0.5	0.6	0.7	0.8
k-factor (Applied stress)	9.27	14.02	18.50	24.46	32.93	44.20	61.00	84.80
Case (A)	22.785	24.855	23.533	23.589	26.501	29.402	41.603	54.892
Case (B)	19.48	24.36	10.41	15.55	27.2	40.56	52.45	60.88
Case (C)	16.27	2.02	-14.00	-26.54	-29.07	-18.30	5.00	42.00
Case (D)	18.06	8.99	-3.65	-10.08	-11.41	-10.33	-4.06	4.50

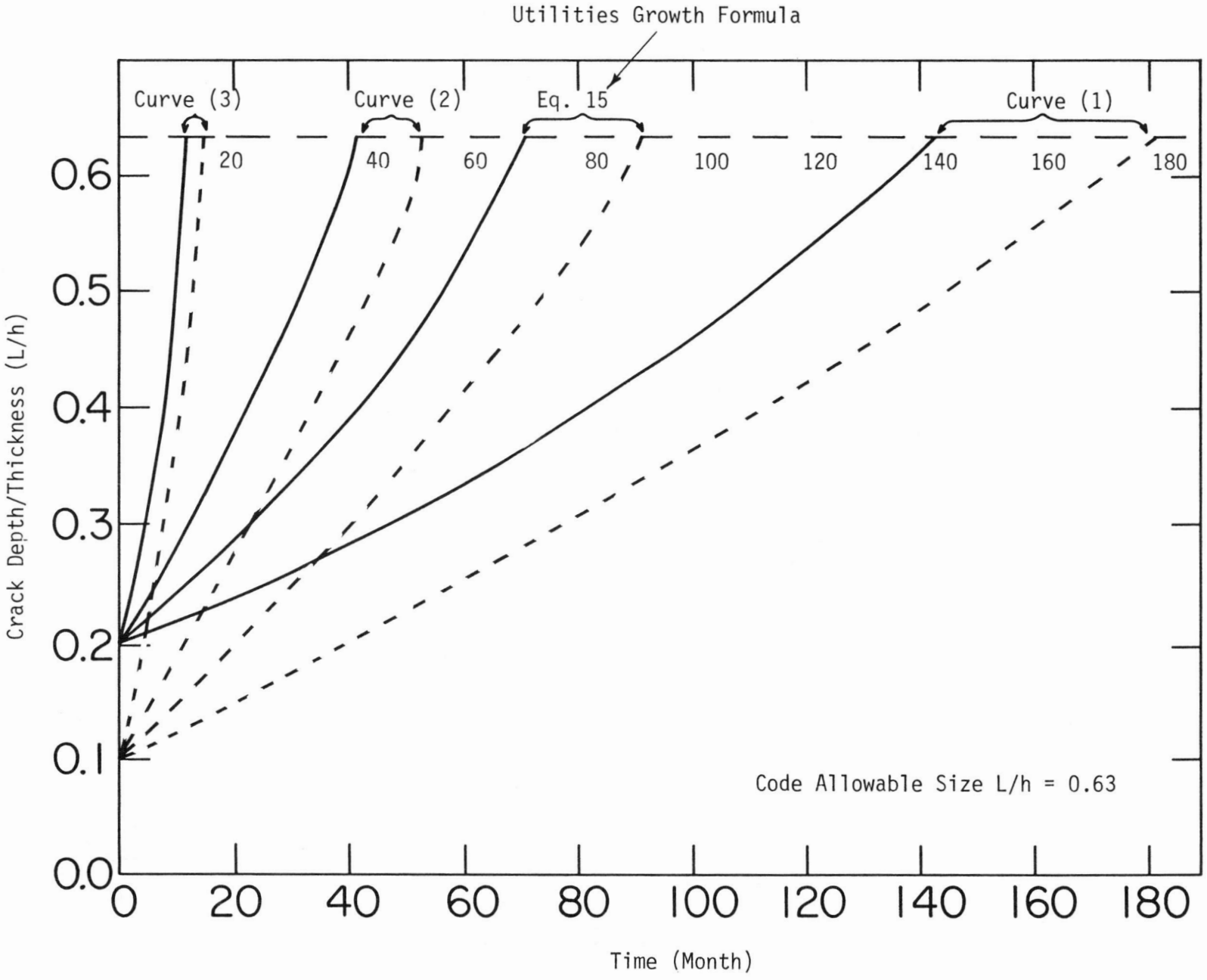

Fig. 22 Crack Growth For 28 in Pipe - Residual Stress Case (A).

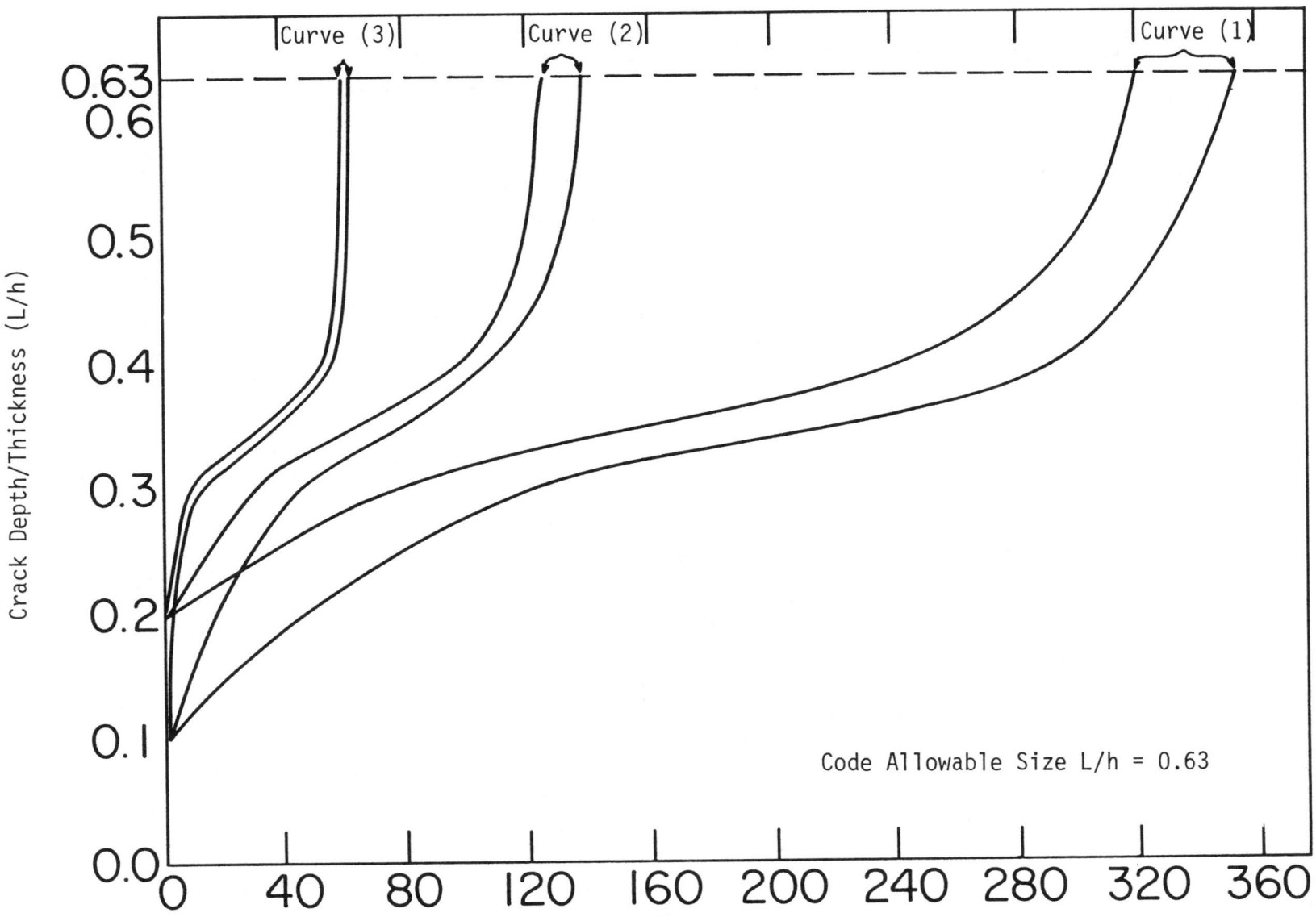

Fig. 23 Crack Growth in 28 in. Pipe - Residual Stress Case (B).

in Figure (23) reveals typical stress corrosion behavior; namely, three-stage development with a long incubation region in the middle followed by rapid growth and penetration through the pipe thickness. It is interesting to note that if the growth formula given in equation (15) is used, the time required for the crack to reach 63% size is larger than that predicted by Curve (1) in Figure (23), i.e., in excess of 360 months. This variation with time, however, is not shown in Figure (23).

Case (C): Consider the residual stress pattern described in Figure (6) which is based upon the strain gauge measurement of Reference [5]. The corresponding stress intensity factors have been obtained by means of integrating the proper influence functions by use of the boundary integral method [5]. The results are shown in the third column of Table (5). The negative k-values in Table (5) are effective in reducing any positive k-factors due to the operating stress levels. Superimposing the k-factors due to residual stress and those due to applied stresses, the total k-factors are obtained as indicated in Table (9). There are negative total k-values in the middle of the pipe wall. This means that the crack will arrest in that region. Thus, if one assumes the residual stress pattern discussed above, the crack can grow up to about (20-25)% of the pipe thickness (over a period exceeding 200 months) and then incubate for a long time afterwards. Thus, the presence of the assumed residual stresses greatly influence the failure probability of the pipe.

Case D: In this case, the stress intensity factors of Table (6), which are based on the residual stress measurements shown in Figure (8) are used to arrive at the total crack driving force. These values are given in Table (9). As in Case (C) discussed previously, the total k-factors in the middle of the pipe thickness are negative and, consequently, any crack indication cannot penetrate that region. Here, again, one can conclude that the assumed highly compressive residual stress in the middle region of the pipe thickness give rise to retarding forces that tend to arrest any crack indication reaching that locality.

Small-Diameter Lines

Because of the nature of the residual stresses in small-diameter BWR lines (0-1 inch wall thickness), crack growth rates are sufficiently fast that immediate repair is recommended if IGSCC is detected by in-service inspection. The residual stress pattern in the smaller line is depicted in Figure (9) and the corresponding k-factors for 4-inch and 12-inch pipes are listed in Table (7). They are completely tensile throughout the pipe wall and, therefore, tend to accelerate crack growth.

The normal operating stress can be taken to be 14 ksi [26]. This is the axial stress due to pressure, thermal expansion and dead weight loading. Besides the ASME Code [25] recommendation, a critical crack depth (for a complete circumferential crack) can also be estimated from the equation

$$\left(\frac{L}{h}\right)_{crit} = 1 - \sigma_{n.o.} / \sigma_f \qquad (22)$$

in which $\sigma_{n.o.}$ stands for the normal operating stress = 14 ksi and σ_f is the flow stress for the austentic material (= 50 ksi). Thus, the critical size is about 70% of the wall thickness.

4-inch pipe: Consider a 4"-pipe with wall thickness h = 0.337 inches, outside diameter = 4.544", and with a normal operating stress of 14 ksi. The total k-factors can be obtained from Table (7) and Section II of this report. The results are given in Table (10). Assume that an in-service inspection of the pipe detects an indication of about 10% of the wall thickness. This indication is located in the heat - affected zone of a weld and, most likely, is a stress corrosion crack and subsequently will propagate. Figure (24) reveals the time needed for this flaw (and another one of size 20% of wall thickness) to penetrate 60% of the pipe thickness. It is readily seen that the slowest growth rate gives a time of about 40 monts while the most conservative law gives a time of less than 5 months.

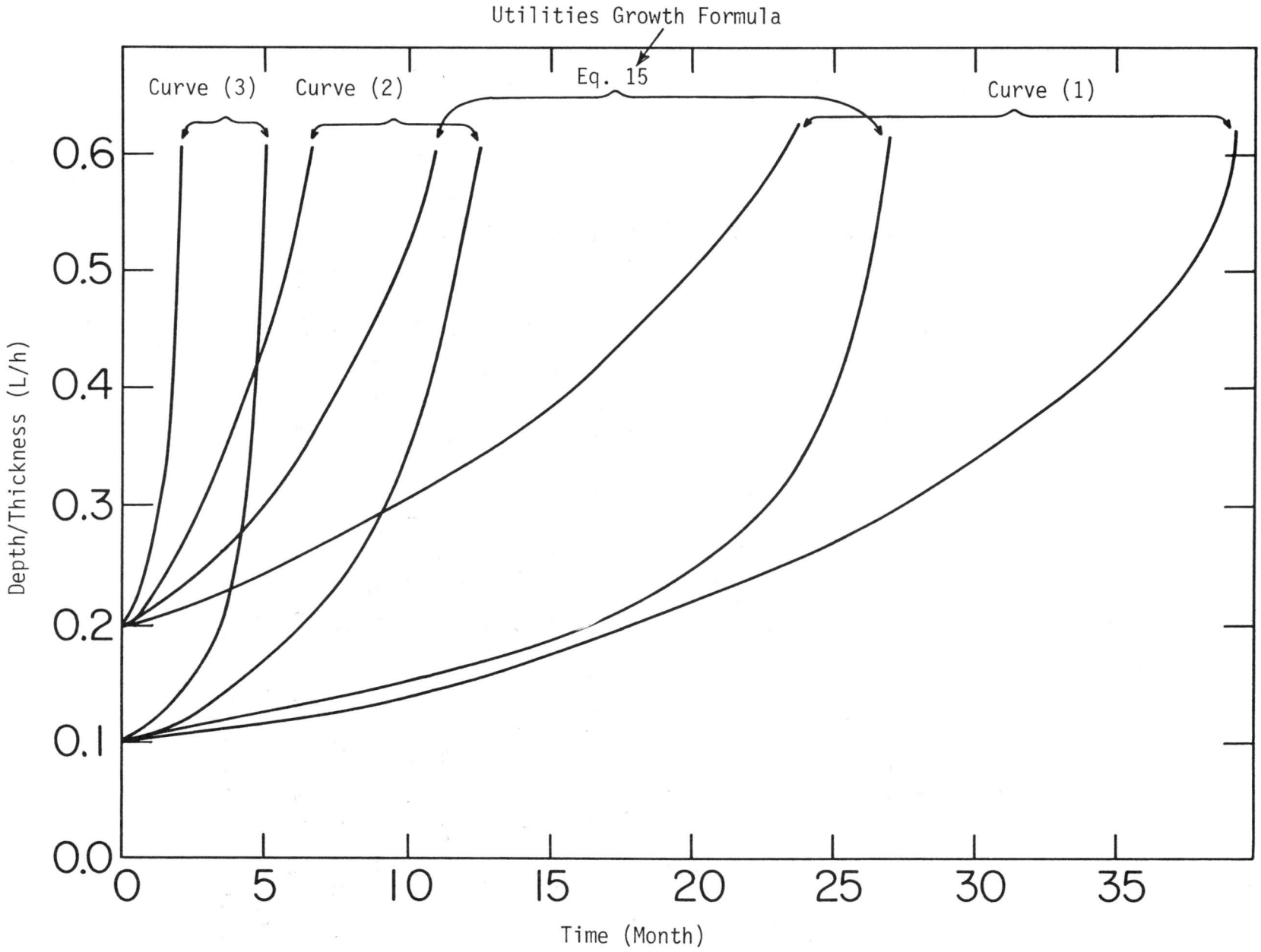

Fig. 24 Crack Growth For 4 in. Pipe.

Suppose that the initially detected flaw has a size of 5% of the wall thickness, then the time needed to propagate to 10% of the thickness, varies between 17 months for the most conservative growth law and 65 months if Equation (15) is assumed for the propagation. Thus, for an initial crack of size = 5% off wall thickness, the time required to reach 60% of the wall thickness lies between 22 months (most conservative growth law) and 105 months (slowest law).

12-inch pipe: For a 12-inch pipe (outside diameter = 12.75 inch, thickness = 0.794 inch) subjected to a normal operating stress (in the axial direction) of 14 ksi, the total values of the stress intensity factors are given in Table (10). Suppose that a pre-existing circumferential flaw has reached a depth of 10% of the pipe thickness. The time needed to propagate to 60% of the pipe thickness is shown in Figure (25). It is clear from Figure (25) that this time varies between 35 months for the slowest growth law and couple of months for the most conservative growth law. A time of about 10 months is needed if one assumes growth laws given in Equations (15) and (19). Figure (25) also displays the time required for an existing flaw of initial size = 20% of the wall thickness to propagate through the wall thickness. The maximum time needed is about 20 months. However, if the initial flaw had penetrated to a depth of 5% then the time needed varies between 57 months for curve (1) and 12 months for curve (3). This indicates that the crack grows rather slowly at first, but then goes through the pipe wall quickly after it reaches 10% - 15% of the wall thickness. Thus for BWR pipes with wall thickness < 1 inch, once stress corrosion cracking has been detected by in-service inspection, immediate repairs should be undertaken to prevent loss of structural integrity of the piping system. It should also be mentioned that for pipes with thickness approaching one inch (i.e., pipes with diameters between 12-inch and 16-inch), the residual stress pattern shown in Figure (9) is rather conservative.

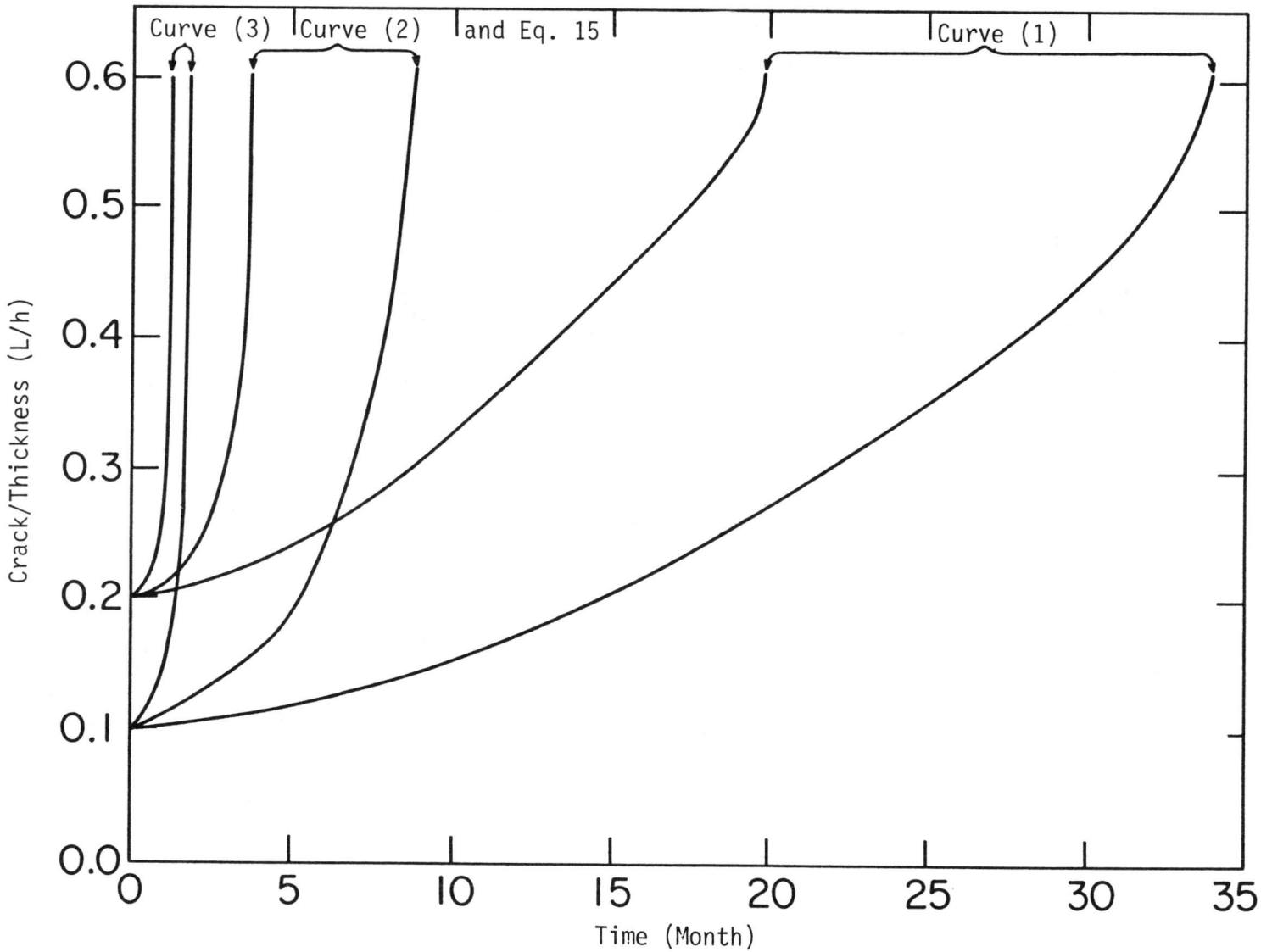

Fig. 25 Crack Growth For 12 in. Pipe.

Table (10): Stress Intensity Factors in Small Diameter Pipes

$\frac{L}{h}$	Total K-Factors (ksi $\sqrt{in}$)	
	4-inch pipe	12-inch pipe
0.1	15.086	23.109
0.2	21.189	32.530
0.3	26.065	40.023
0.4	30.511	46.848
0.5	35.874	55.082
0.6	38.440	59.020
0.7	45.227	69.439
0.8	46.773	71.815

V. SUMMARY COMMENTS

This report presents the results of a study conducted to evaluate the effects of stress intensity factor and environment on the growth behavior of intergranular stress corrosion cracks in type 304 stainless steel piping systems. Most of the detected cracks are known to be circumferential in shape, and initially start at the inside surface in the heat affected zone near girth welds. These cracks grow both radially in-depth and circumferentially in length and, in extreme cases, may cause leakage in the installation. The propagation of the crack is essentially due to the influence of the following simultaneous factors: (1) The action of applied and residual stress, (2) Sensitization of the base metal in the heat affected zone adjacent to girth weld and (3) The continuous exposure of the material to an aggressive environment of high temperature water containing dissolved oxygen and some levels of impurities.

The first task in investigating the behavior of crack growth focused on reviewing the published literature in order to determine the crack driving force as measured by the stress intensity factor (k-factor) under normal and extreme service conditions. This is accomplished in Section II where a comprehensive compilation of formulas and numerical values of the relevant k-factors, obtained by various elastic techniques, is presented and discussed. Included in this section are k-factors for complete circumferential cracks, long axial cracks and semi-elliptical part-through axial and circumferential cracks. Upon examination of the given values, it is clear that the k-factors of a partial circumferential crack in a pipe is always less than the corresponding values (for the same loading) of a complete circumferential crack. Hence, the use of the latter would yield conservative growth characteristics. Several k-factors for typical distributions of residual stresses in large and small diameter pipes are calculated and, where possible, the results are compared with available ones in the literature. It is apparent that the magnitude and distribution of residual stress across the pipe thickness have a major influence on crack growth. For large diameter pipes (thickness > 1"),

the accepted pattern of residual stress gives rise to negative k-factor of large magnitude in the middle region of the wall thickness. This value when superimposed upon the k-factor due to the applied stress has the helpful effect of mitigating or even arresting crack growth in that region of the wall. On the other hand, for small diameter pipes (thickness < 1"), the opposite effect occurs since the residual stress give rise to tensile k-factors throughout the pipe thickness. This has the effect of accelerating crack growth. The transition between the k-factors for large and small diameter pipes seems to occur for pipes with wall thickness = 1 inch (i.e., 12 -inch to 16-inch pipes). The authors are of the opinion that the small-ameter pattern of residual stress for 12-inch to 16-inch pipes are on the conservative side.

Residual stresses that might exist tangential to the crack plane have been neglected in this study. Whether such stresses exist or not and what is their role on crack growth is an open question. Moreover, for residual stresses to exist, the state of stress is fundamentally non-linear. However, for reason of simplicity, linear superposition of the applied stress k-factors on the corresponding k-factors due to residual stresses is adopted in this report as is customarily done in the literature. The ramification of this assumption is open to discussion.

Section III of this report contains a number of crack growth laws developed from the available experimental data. Of particular interest is an upper bound power law derived from the envelope which contain all the relevant data to depict the crack growth rate. The use of such a law would assure the most conservative estimate of crack movement. Additional crack growth formulas are also given to predict results which are in reasonable agreement with actual field behavior. The most important factor affecting the crack growth rate is the level of sensitization present in the material at the heat affected zone near the weld joints where intergranular cracks are situated. Sensitization depends on the sensitizing heat treatment (during the welding process) and on the material carbon content. Faster crack growth (almost by

an order of magnitude) can be developed by applying a high degree of sensitization to the same specimen assuming all other factors are identical. Thus, it is essential to have a reliable knowledge of the actual degree of sensitization in the field pipe before the predictive methodology can be applied to determine the subcritical life of stress corrosion cracks. An important question which does not seem to have been addressed in the literature is this: How reliable the test data are when applied to predict actual crack growth behavior in field pipes? In other words, what is the influence of size or scaling effects? Since the experimental data generated are based on cracking small size specimens, how can one be sure that the data applies to actual pipes in the field? To answer this question properly, one must compare the data generated from testing small specimens with the results of testing actual size pipes. The pipes should be subjected to the same distortions and environment as in BWR installations which is difficult to duplicate in the laboratory. To the best knowledge of the authors, no definitive data are available in the open literature, although some scattered data is available [27] and additional work is currently in progress towards achieving this aim [21]. Moreover, it should be pointed out that the fracture mechanics growth formulas are based on having "k-controlled" crack tip in the specimen and in the field. In reality, the crack tip is in a plastically deformed material in both the specimen and field pipe. Does this lead to different growth time than the one predicted by the growth formula? The authors are of the opinion that it does not and, barring any significant scaling effect, the assumption that the rate of crack growth is a function of the stress intensity factor is a reasonable conjucture.

In Section IV, the time required for hypothetical cracks in BWR pipes to propagate to their critical size is computed and displayed graphically. A parametric study is performed in order to assess the relative influence and sensitivity of the various input parameters (residual stress, crack growth law, diameter of pipe, initial size of defect, etc.) which have bearing on the growth behavior of the intergranular stress corrosion cracks in type 304 stainless steel. Cracks in large-diameter as well as in small-diameter pipes are considered and analyzed.

VI. CONCLUSIONS

The major accomplishments and conclusions reached in this study are:

(1) Stress Intensity Factors: The available techniques and formulations for computing the stress intensity factors of surface cracks in pipes were reviewed and assembled in the report. The assembled data included k-factors for both full- and part-circumferential cracks as well as axial cracks. For identical loadings the k-factor of a partial-circumferential crack is always less than the corresponding value of the complete circumferential crack. Thus, the use of the latter value will insure conservative growth characteristics for these types of cracks.

(2) Operating Stress: Crack growth depends on the combination of k-factors due to operating and residual stresses. As long as the sum is positive there will be crack growth. For this study typical operating stress values for various pipe sizes given in the literature were used for crack growth calculations. Variations of operating stress and their effects on the crack growth in representative piping systems are being studied.

(3) Residual Stress and Pipe Geometry Effects: The pattern of residual stress distribution across the thickness due to welding has a major influence on crack growth. For large diameter pipes (diameter 26-28" with thickness 1-3/8"), significant variations in the residual stress distribution have been reported. As discussed in the text, for some distributions the total k-factor can become negative at some crack depth and thus arrest further crack growth. For other distributions of residual stress, however, there is continuous crack growth (see Figs. 22 and 23), with varying time estimates to code allowable crack size depending on initial crack depth and applied crack growth law. It is the authors opinion, that the latter residual stress distributions are more realistic, and complete crack arrest in unlikely to occur. As can be observed from the above mentioned figures, for detected flaws with initial depth to thickness ratios of 10 to 20 percent, there is a large range for the predicted life. Considering only the average crack growth laws, the predicted life to code allowable size, would range from approximately 40 to 100 months, while the most conservative crack growth law would yield a time range of 10 to 60

months. For deeper initial cracks, lifetimes will be shorter and time ranges due to different residual stress assumptions will also be less. These factors must be considered in order to establish an effective inspection and repair schedule.

In small diameter pipes available data indicates that the residual stress always has an aggravating effect, in that it accelerates crack growth. Life estimates for these pipes are displayed in figures 24 and 25. From the results, it is recommended that these pipes be repaired or replaced as soon as flaws are detected.

(4) Environment and Water Chemistry: The degree of sensitization in the base metal near a weld joint (where intergranular cracks are detected) has a great influence on the expected time for subcritical crack growth. Faster growth (by an order of magnitude or higher) has been achieved in the laboratory by utilizing test specimens with a higher level of sensitization. There is some data which suggests that the degree of sensitization in a weld joint of an operating BWR pipe increases with time and can lead to accelerated cracking.

The amount of dissolved O_2 concentration influences crack growth rate when it is below 1 ppm but does not seem to have an affect above that level. In addition, there is evidence which indicates that dilute levels of impurities (sulfates and chlorides) present in the water can increase growth time.

Recommendations

The above accomplishments and conclusions are based on the original work scope envisioned for this task. Based on the outcome of this study, the following recommendations can be made:

(1) As detailed in the report, the distribution of the weld residual stress across the thickness in large diameter pipes cannot be adequately determined from existing literature data. Considering that crack growth or its arrest is greatly influenced by the residual stress k-factor, it is recommended that a detailed analytical study be carried out to determine the important parameters affecting the residual stress distributions and their corresponding k-factors.

Furthermore, a review should be made of experimental methods that would allow the determination of actual residual stresses. When combined with the metallurgical aspects, this study could result in the identification of the most optimum welding conditions that would lead to favorable residual stress distributions and degree of material sensitization.

(2) Weld overlays were not included in this phase of the BNL Work Scope. Since this technique (which again involves weld residual stresses) is one of the major components of the repair program, its effects with respect to stress redistribution and consequent crack growth or arrest need detailed study.

(3) In the study k-factors for fully circumferential cracks were used in order to obtain conservative time estimates for growth. Some calculations using k-factors for partially circumferential cracks should also be made for comparative purposes.

(4) As mentioned, typical operating stress values for various pipe sizes were taken from the literature. In order to evaluate the variations inherent in the operating stresses and their effects on crack growth, it is recommended that a stress calculation be performed for a typical piping system. This is a relatively simple and straight forward task if piping system data is available.

REFERENCES

1. H.F. Nied and F. Erdogan, "The Elasticity Problem for a Thick-Walled Cylinder Containing a Circumferential Crack", International Journal of Fracture", Vol. 22, 1983, pp. 277-301.

2. P.C. Paris and G.C. Sih, "Stress Analysis of Cracks", Symposium on Fracture Toughness Testing and its Applications", ASTM - STP No. 381, 1965, Philadelphia, PA.

3. M.K. Kassir and G.C. Sih, Three Dimensional Crack Problems, Noordhoff International Publishing, Leyden, The Netherlands, 1975.

4. R. Labbens, A. Pellisier-Tanon and J. Heliot, "Practical Method for Calculating Stress-Intensity Factors Through Weight Functions", Mechanics of Crack Growth, ASTM Special Technical Publications, No. 590, 1976, pp. 368-384, Philadelphia, PA.

5. D.O. Harris, "The Influence of Crack Growth Kinetics and Inspection on the Integrity of Sensitized BWR Piping Welds", EPRI NP-1163, September 1979. See also ASTM STP 743, 1981, pp. 375-386.

6. E-F. Ribicki, P.M. McGuire and R.B. Stonesifer, "Effect of Weld Parameters on Residual Stresses in Boilng Water Reactor Piping Systems", First Semi-Annual Progress Report, April 1, 1978, RP 1174, EPRI, Palo Alto, CA.

7. W.J. Shack, W.A. Ellingson and L.E. Pahis, "The Measurement of Residual Stresses in Type 304 Stainless Steel Piping Butt Weldments", EPRI RP 449-1, December 1978, Palo Alto, CA, (See also EPRI Report NP-1413, June 1980).

8. D.D. Dedhia and D.O. Harris, "Stress-Intensity Factors for Surface Cracks in Pipes: A Computer Code for Evaluations by Use of Influence Functions", EPRI NP-2425, June 1982, Palo Alto, CA.

9. C.B. Buchalet and W.H. Bamford, "Stress Intensity Factor Solution for Continuous Surface Flaws in Reactor Pressure Vessels", Mechanics of Crack Growth, ASTM SPT 590, 1976, pp. 385-402.

10. S. Ranganath and D.M. Norris, "Evaluation Procedure and Acceptance Criteria for Flaws in Austenitic Steel Piping", Report submitted by BWR Owners Group Representative to NRC, July 5, 1983.

11. H.L. Gustin, et al., "Design Report for Weld Overload Repairs and Flaw Evaluation in Recirculation and RHR Systems at Georgia Power Company's E.I. Hatch Nuclear Power Plant, Unit 2", prepared by Nuctech Engineers, Inc., San Jose, CA, June 1983.

12. J. Helist, R.C. Labbens and A. Pellisier, "Semi-Elliptical Cracks in a Cylinder Subjected to Stress Gradients", Fracture Mechanics, ASTM SPT 677, 1979, pp. 341-364.

13. J.C. Newman and I.S. Raju, "Stress Intensity Factors for Internal Surface Cracks in Cylindrical Pressure Vessels", NASA Technical Memorandum 80073 (July 1979).

14. J.J. Mcgowan and M. Raymund, "Stress Intensity Factor Solutions for Internal Longitudinal Semi-Elliptical Surface Flaws in a Cylinder Under Arbitrary Loadings", Fracture Mechanics, ASTM STP 677, 1979, pp. 365-380.

15. Kobayashi, A.S., Emery, A.F., Polranich, N. and Love, W.J., "Surface Flaw in a Pressurized and Thermally Shocked Hollow Cylinder", International Journal of Pressure Vessels and Piping, Vol. 5, 1977, pp. 103-122.

16. Smith, C.W. Peters, W.H., Hardrath, W.T. and Fleischman, T.S., "Stress Intensity Distributions in Nozzle Corner Cracks of Complex Geometry", Transactions of 5th International Conference on Structural Mechanics in Reactor Technology, Paper No. G4/4, 1979.

17. M.J. Povich, "Low Temperature Sensitization of Type 304 Stainless Steel", Corrosion, Vol. 34, No. 2, 1978, pp. 60-64.

18. M.J. Povich and P. Rao, "Low Temperature of Welded Type 304 Stainless Steel", Corrosion, Vol. 34, No. 8, 1978, pp. 269-275.

19. R. Huet, L.C. Hsu, D.A. Gerber and P.C. Riccandella, "Stress Corrosion Cracking of Type 304 Stainless Steel in High-Purity Water: A Compilation of Crack Growth Rates", EPRI Report NP-2423-LO, Palo Alto, CA, June 1982.

20. F.P. Ford and M. Silverman, "Effect of Load Rate on Environmentally Controlled Cracking of Sensitized 304 Stainless Steel in High Purity Water", Corrosion, Vol. 36, No. 11, 1980, pp. 597-603.

21. R.M. Horn, et al., "The Growth and Stability of Stress Corrosion Cracks in Large Diameter BWR Piping", General Electric Report NEDC-27450-3, December 1980.

22. R.M. Horn, Editor, "The Growth and Stability of Stress Corrosion Cracks in Large-Diameter BWR Piping", EPRI Report NP-2472-54-SY (Vol. 1: Summary; Vol. 2: Appendices), July 1982.

23. W. Shack, Argonne National Laboratory, Private Communication, October 1983.

24. T.F. Kassner, Argonne National Laboratory, Private Communication, October 1983.

25. ASME Boiler and Pressure Vessel Code Section XI, Paragraph IWB-3640, "Acceptance Criteria for Austenitic Stainless Steel Piping".

26. General Electric Stress Report 22A-4264.

27. R.L. Brickford, "Twenty Six-Inch Pipe NDE Instrument Surveillance Test", EPRI Interim Report NP-2869, Research Project T 104-1, February 1983.